

**COMPARISON OF DESIGN SPECIFICATIONS
FOR
SEISMICALLY ISOLATED BUILDINGS**

**A THESIS SUBMITTED TO
THE GRADUATE SCHOOL OF NATURAL AND APPLIED SCIENCES
OF
MIDDLE EAST TECHNICAL UNIVERSITY**

**BY
EMRE ACAR**

**IN PARTIAL FULFILLMENT OF THE REQUIREMENTS
FOR
THE DEGREE OF MASTER OF SCIENCE
IN
CIVIL ENGINEERING**

FEBRUARY 2006

Approval of the Graduate School of Natural and Applied Sciences

Prof. Dr. Canan Özgen
Director

I certify that this thesis satisfies all the requirements as a thesis for the degree of
Master of Science.

Prof. Dr. Erdal Çokca
Head of Department

This is to certify that we have read this thesis and that in our opinion it is fully
adequate, in scope and quality, as a thesis for the degree of Master of Science.

Assoc. Prof. Dr. Uğurhan Akyüz
Supervisor

Examining Committee Members

Prof. Dr. S. Tanvir Wasti (METU, CE) _____

Assoc. Prof. Dr. Uğurhan Akyüz (METU, CE) _____

Assoc. Prof. Dr. Ahmet Yakut (METU, CE) _____

Asst. Prof. Dr. Ahmet Türer (METU, CE) _____

M.Sc. Mevlüt Kahraman (ÇEVİKLER İNŞAAT) _____

I hereby declare that all information in this document has been obtained and presented in accordance with academic rules and ethical conduct. I also declare that, as required by these rules and conduct, I have fully cited and referenced all material and results that are not original to this work.

Name, Last name: Emre Acar

Signature :

ABSTRACT

COMPARISON OF DESIGN SPECIFICATIONS FOR SEISMICALLY ISOLATED BUILDINGS

Acar, Emre

M. Sc., Department of Civil Engineering

Supervisor: Assoc. Prof. Dr. Uğurhan Akyüz

February 2006, 103 pages

This study presents information on the design procedure of seismic base isolation systems. Analysis of the seismic responses of isolated structures, which is oriented to give a clear understanding of the effect of base isolation on the nature of the structure; and discussion of various isolator types are involved in this work.

Seismic isolation consists essentially of the installation of mechanisms, which decouple the structure, and its contents, from potentially damaging earthquake induced ground motions. This decoupling is achieved by increasing the horizontal flexibility of the system, together with providing appropriate damping. The isolator increases the natural period of the overall structure and hence decreases its acceleration response to earthquake-generated vibrations. This increase in period,

together with damping, can reduce the effect of the earthquakes, so that smaller loads and deformations are imposed on the structure and its components.

The key references that are used in this study are the related chapters of FEMA and IBC2000 codes for seismic isolated structures. In this work, these codes are used for the design examples of elastomeric bearings. Furthermore, the internal forces develop in the superstructure during a ground motion is determined; and the different approaches defined by the codes towards the ‘scaling factor’ concept is compared in this perspective.

Keywords: Seismic Isolation, Base Isolation, Earthquake Resistant Design, Seismic Protective Systems

ÖZ

SİSMİK İZOLASYONLU BİNALAR İÇİN DİZAYN ŞARTNAMESLERİNİN KİYASLANMASI

Acar, Emre

Yüksek Lisans, İnşaat Mühendisliği Bölümü

Tez Yöneticisi: Doç. Dr. Uğurhan Akyüz

Şubat 2006, 103 sayfa

Bu çalışma sismik taban izolasyon sistemlerinin dizayn prosedürü hakkında bilgi sunmaktadır. Taban izolasyonunun yapının davranışı üzerindeki etkisinin net bir biçimde anlaşılabilmesi amacıyla, izole edilmiş yapıların sismik davranışlarının analizi; ve çeşitli izalatör tiplerinin tartışması bu çalışmada mevcuttur.

Sismik izolasyon esasen yapıyı ve içindekileri hasar verici potansiyel depremin neden olduğu yer hareketlerinden ayrıştıran mekanizmaların yerleştirilmesinden oluşur. Bu ayrıştırma yeterli miktarda sönümlenme ile birlikte sistemin yatay esnekliğinin arttırılması ile gerçekleştirilir. İzolatörler tüm yapının doğal periyodunu yükseltir ve dolayısıyla deprem kaynaklı titreşimlere cevaben yapıda oluşan ivmelenme azalır. Periyottaki bu artış, sönümlenme ile birlikte, depremin etkisini

farkedilir bir biçimde azaltır; yani yapıya ve bileşenlerine daha az yıkıcı kuvvetler ve deformasyonlar etki eder.

Bu çalışmada kullanılan anahtar referanslar FEMA ve IBC2000 kodlarının yapıların sismik izolasyonu ile ilgili bölümleridir. Bu çalışmada bu kodlar elastomer mesnetlerin örnek dizaynında kullanılmıştır. Bunun yanısıra yer hareketi esnasında üstyapıda oluşan dizayn yükleri belirlenmiş ve kodların ‘derecelendirme faktörü’ kavramına olan farklı yaklaşımları bu açıdan kıyaslanmıştır.

Anahtar Kelimeler: Sismik İzolasyon, Taban İzolasyonu, Depreme Dayanıklı Yapı Dizaynı, Sismik Koruyucu Sistemler

Dedicated to my parents, Güler and Eyüp Acar,
for their presence and encouragement.

ACKNOWLEDGMENTS

I would like to express my sincere gratitude to the following:

Assoc. Prof. Dr. Uğurhan Akyüz, my thesis supervisor, for his proper directives and close interest without which this work would never be realized,

My family for their ineffable guidance, motivation and constant support,

Finally, my love, Özlem İlhan, for patiently enduring and sharing the years of preparation with me.

TABLE OF CONTENTS

PLAGIARISM.....	iii
ABSTRACT.....	iv
ÖZ.....	vi
ACKNOWLEDGEMENTS.....	ix
TABLE OF CONTENTS.....	x
LIST OF FIGURES.....	xiii
LIST OF TABLES.....	xvi
LIST OF SYMBOLS.....	xviii

CHAPTER

1. INTRODUCTION.....	1
1.1 Principles of Seismic Isolation.....	2
1.2 Seismic Isolation Systems.....	4
1.2.1 Elastomeric Bearings.....	4
1.2.1.1 Low Damping Natural and Synthetic Rubber Bearings.....	4
1.2.1.2 High Damping Natural Rubber Bearings.....	5
1.2.1.3 Lead-Plug Bearings.....	6
1.2.2 Isolation Systems Based on Sliding.....	7
1.2.2.1 Pure-Friction System.....	8
1.2.2.2 Resilient-Friction Base Isolation System.....	8
1.2.2.3 Electric de France System.....	9
1.2.2.4 Friction Pendulum System.....	10
1.3 Current Applications.....	11

1.4	Literature Survey.....	14
1.5	Aims and Scope.....	16
2.	MATHEMATICAL MODELLING OF ISOLATORS.....	17
2.1	Mechanical Characteristics of Elastomeric Isolators.....	17
2.1.1	Comparison of Compression Modulus.....	18
2.2	Equivalent Linear Model of Isolators.....	21
2.3	Bilinear Model of Isolators.....	22
2.4	Comparison of Response for Bilinear and Equivalent Linear Model.....	24
3.	CASE STUDIES.....	37
3.1	Introduction.....	37
3.2	Description of the Structures.....	37
3.2.1	Three-Storey Symmetrical Building (Type-I).....	38
3.2.2	Five-Storey Symmetrical Building (Type-II).....	39
3.2.3	Eight-Storey Symmetrical Building (Type-III).....	40
3.2.4	Non-symmetrical Building (Type-IV).....	40
3.3	Analysis Methods.....	42
3.3.1	Static Equivalent Lateral Force Procedure.....	42
3.3.2	Response Spectrum Analysis.....	45
3.3.3	Time History Analysis.....	46
3.4	Design Codes.....	46
3.4.1	IBC2000.....	47
3.4.2	FEMA273.....	49
4.	ISOLATION SYSTEM DESIGN.....	50
4.1	Design of High Damping Rubber Bearing.....	50
4.1.1	Lateral Stiffness of Base Isolators.....	51
4.1.2	Estimation of Lateral Displacements.....	52
4.1.3	Estimation of Disc Dimensions.....	52
4.1.4	Actual Bearing Stiffness & Revised Fundamental Period.....	53
4.1.5	Bearing Detail.....	53

4.1.6	Buckling Load.....	55
4.2	Performance Comparison of Isolation Systems.....	56
5.	ANALYSIS AND DISCUSSION OF RESULTS.....	61
5.1	Analysis of the Base Isolated Symmetrical Building.....	61
5.1.1	Scaling of the Results	61
5.1.1.1	Scaling for Static Equivalent Lateral Force Procedure	62
5.1.1.2	Scaling for Response Spectrum Analysis.....	63
5.1.1.3	Scaling for Time History Analysis.....	65
5.1.2	Results of the Analyses	67
5.2	Analysis of the Base Isolated Non-symmetrical Building.....	80
5.2.1	Scaling of the Results	80
5.2.1.1	Scaling for Static Equivalent Lateral Force Procedure	80
5.2.1.2	Scaling for Response Spectrum Analysis.....	81
5.2.1.3	Scaling for Time History Analysis.....	83
5.2.2	Results of the Analyses.....	84
5.3	Comparison of FEMA and IBC2000.....	94
5.3.1	Equivalent Lateral Load Analysis.....	95
5.3.2	Response Spectrum Analysis.....	95
5.3.3	Time History Analysis.....	96
6.	CONCLUSION.....	99
	REFERENCES.....	101

LIST OF FIGURES

FIGURES	Page
1.1 Acceleration response spectrum.....	2
1.2 Displacement response spectrum.....	3
1.3 High damping rubber bearing.....	6
1.4 Lead-Plug bearing.....	7
1.5 Resilient-friction base isolation system.....	9
1.6 Friction pendulum system.....	11
2.1 $E_c - S$ relationship.....	20
2.2 $E_c - G$ relationship.....	20
2.3 $E_c - K$ relationship.....	21
2.4 Force displacement relationship of equivalent linear model.....	22
2.5 Force displacement relationship of bilinear model.....	23
2.6 Acceleration spectra.....	24
2.7 Displacement spectra.....	25
2.8 Time variation of top floor acceleration under the effect of Imperial Valley 1979 earthquake.....	29
2.9 Time variation of bearing displacement under the effect of Imperial Valley 1979 earthquake.....	30
2.10 Time variation of top floor acceleration under the effect of Kocaeli 1999 earthquake.....	31
2.11 Time variation of bearing displacement under the effect of Kocaeli 1999 earthquake.....	32
2.12 Time variation of top floor acceleration under the effect of Loma Prieta 1989 earthquake.....	33
2.13 Time variation of bearing displacement under the effect of Loma Prieta 1989 earthquake.....	34

2.14	Force-deformation behavior for Imperial Valley Earthquake (bilinear hysteretic models).....	35
2.15	Force-deformation behavior for Kocaeli Earthquake (bilinear hysteretic models).....	35
2.16	Force-deformation behavior for Loma Prieta Earthquake (bilinear hysteretic models).....	36
3.1	Plan view of symmetrical building types.....	38
3.2	Section view building Type-I.....	39
3.3	Section view of building Type-II.....	39
3.4	Section view of building Type-III.....	40
3.5	Plan view of building Type-IV.....	41
3.6	Section views of building Type-IV.....	41
3.7	Plan dimensions for calculation of D_{TD}	44
3.8	Response spectrum functions given in Turkish Seismic Code.....	44
4.1	Detail design of isolator.....	55
4.2	Effect of damping for equal base shear case.....	58
4.3	Effect of damping for equal period case.....	59
4.4	Effect of damping for equal displacement case.....	60
5.1	Base shear in X direction (Type-II, time history analysis).....	73
5.2	Base shear in Y direction (Type-II, time history analysis).....	74
5.3	Base moment in X direction (Type-II, time history analysis).....	74
5.4	Base moment in Y direction (Type-II, time history analysis).....	75
5.5	Maximum interstory drift ratio (Type-II, time history analysis).....	76
5.6	Base shear in X direction (Type-II, response spectrum analysis).....	76
5.7	Base shear in Y direction (Type-II, response spectrum analysis).....	77
5.8	Base moment in X direction (Type-II, response spectrum analysis).....	78
5.9	Base moment in Y direction (Type-II, response spectrum analysis).....	78
5.10	Maximum interstory drift ratio (Type-II, response spectrum analysis).....	79
5.11	Base shear in X direction (Type-IV, time history analysis).....	88
5.12	Base shear in Y direction (Type-IV, time history analysis).....	89
5.13	Base moment in X direction (Type-IV, time history analysis).....	89
5.14	Base moment in Y direction (Type-IV, time history analysis).....	90

5.15	Maximum interstory drift ratio (Type-IV, time history analysis).....	91
5.16	Base shear in X direction (Type-IV, response spectrum analysis).....	91
5.17	Base shear in Y direction (Type-IV, response spectrum analysis).....	92
5.18	Base moment in X direction (Type-IV, response spectrum analysis).....	93
5.19	Base moment in Y direction (Type-IV, response spectrum analysis).....	93
5.20	Maximum interstory drift ratio (Type-IV, response spectrum analysis).....	94

LIST OF TABLES

TABLES	Page
1.1 Current applications of seismic isolation.....	13
2.1 The parameters of bilinear hysteresis loop.....	26
2.2 Results of the analyses.....	27
3.1 Damping coefficient.....	42
3.2 Ground motions used in time history analyses.....	46
3.3 Scaling limits for IBC2000.....	49
5.1 Calculation of scaling factor for Type-II according to IBC2000.....	62
5.2 Fixed and isolated periods of buildings.....	63
5.3 Calculation of scaling factor for Type-I according to IBC2000.....	64
5.4 Calculation of scaling factor for Type-II according to IBC2000.....	64
5.5 Calculation of scaling factor for Type-III according to IBC2000.....	64
5.6 Calculation of scaling factor for Type-I according to FEMA.....	65
5.7 Calculation of scaling factor for Type-II according to FEMA.....	65
5.8 Calculation of scaling factor for Type-III according to FEMA.....	65
5.9 Calculation of scaling factor for Type-II according to IBC2000.....	66
5.10 Calculation of scaling factor for Type-II according to FEMA.....	67
5.11 Results of the analyses for Type-II.....	68
5.12 Comparison Table for Type-II.....	69
5.13 Results of time history analysis for each earthquake record, Type-II.....	70
5.14 Calculation of scaling factor for Type-IV according to IBC.....	79
5.15 Fixed and isolated periods.....	79
5.16 Calculation of scaling factor for Type-IV according to IBC2000.....	80
5.17 Calculation of scaling factor for Type-IV according to FEMA.....	81

5.18	Calculation of scaling factor for Type-IV according to IBC2000.....	82
5.19	Calculation of scaling factor for Type-IV according to FEMA.....	82
5.20	Results of the analyses for Type-IV.....	83
5.21	Comparison Table for Type-IV.....	84
5.22	Results of time history analysis for each earthquake record, Type-IV.....	85

LIST OF SYMBOLS

A	Cross-sectional area
A_0	Seismic zone coefficient
B_D	Numerical coefficient for effective damping at design displacement
b	Long side length of building in plan
D	Specified design displacement
D_y	Yield displacement
D_D	Displacement corresponding to the ‘design earthquake’
D_{TD}	Total design displacement
D_M	Displacement corresponding to the ‘max. capable earthquake’
d	Short side length of building in plan
e	Eccentricity
E_{loop}	Energy dissipation per cycle of loading
E_c	Instantaneous compression modulus
F^+	Positive force at test displacement
F^-	Negative force at test displacement
$(F_v)_{max}$	Maximum vertical load for one isolator
G	Shear modulus of the elastomer
g	Acceleration of gravity
h	Total height of bearing
h_i	Height above the base to level i
h_x	Height above the base to level x
I	Importance factor of structure
K_H	Horizontal stiffness of bearing

K_V	Vertical stiffness of bearing
K	Bulk modulus
K_1	Elastic stiffness
K_2	Post-yield stiffness
k_{eff}	Effective stiffness
k_D	Lateral stiffness corresponding to the ‘design earthquake’
k_M	Lateral stiffness corresponding to the ‘max. capable earthquake’
M_W	Magnitude
N	Number of storey
Q	Characteristic strength
P_{cr}	Critical buckling load
P_E	Euler buckling load
P_S	Shear stiffness per unit length
R	Seismic load reduction factor
S	Shape factor
S_{D1}	Design 5% damped spectral acceleration at 1 sec. Period
T	Fixed-based period
T_M	Isolated period at maximum displacement
T_{eff}	Effective period
T_D	Isolated period at design displacement
T_V	Vertical fundamental period of vibration
t_r	Total thickness of rubber
t_o	Thickness of single layer of rubber
W_D	Area of hysteresis loop
W_x	Portion of W that is located at or assigned to level x
W_i	Portion of W that is located at or assigned to level i
W	Total weight of superstructure
V_S	Base shear force
β	Damping ratio
β_{eff}	Effective viscous damping ratio

β_s	Damping ratio of superstructure
β_i	Damping ratio of isolator
Δ^+	Positive peak test displacements
Δ^-	Negative peak test displacements
γ_{\max}	Maximum shear strain
Φ	Diameter

CHAPTER 1

INTRODUCTION

Seismic isolation, also known as base isolation in structures, is an innovative design strategy that provides a practical alternate for the earthquake resistant design of new structures and the seismic rehabilitation of existing buildings, bridges and industrial establishments. The concept of seismic isolation is based on the premise that a structure can be substantially decoupled from damaging horizontal components of earthquake ground motions. Thus, earthquake induced forces may be reduced by factors of five to ten from those that a conventional fixed-base structure would experience.

During earthquake attacks, the traditional building structures in which the base is fixed to the ground, respond with a gradual increase from ground level to the top of the building, like an amplifier. This may result in heavy damage or total collapse of structures. To avoid these results, while at the same time satisfying in-service functional requirements, flexibility is introduced at the base of the structure, usually by placing elastomeric isolators between the structure and its foundation. Additional damping is also needed to control the relative displacement between the structure and the ground.

1.1. Principles of Seismic Isolation

Seismic isolation is a design approach aimed at protecting structures against damage from earthquakes by limiting the earthquake attack rather than resisting it. In seismically base-isolated systems, the superstructure is decoupled from the ground motion by introducing horizontally flexible but vertically very stiff components at the base level of the structure. Thereby, the isolation system shifts the fundamental time period of the structure to a large value and/or dissipates the energy in damping, limiting the amount of force that can be transferred to the superstructure such that interstory drift and floor accelerations are reduced drastically.

Typical earthquake accelerations have dominant periods of about 0.1-1.0 sec. with maximum severity often in the range 0.2-0.6 sec. Structures whose natural periods of vibration lie with in the range 0.1-1.0 sec. are therefore particularly vulnerable to seismic attacks because they may resonate. The most important feature of seismic isolation is that its increased flexibility increases the natural period of the structure (>1.5 sec., usually 2.0-3.0 sec.). Because the period is increased beyond that of the earthquake, resonance is avoided and the seismic acceleration response is reduced [22]. The benefits of adding a horizontally compliant system at the foundation level of a building can be seen in Figure 1.1.

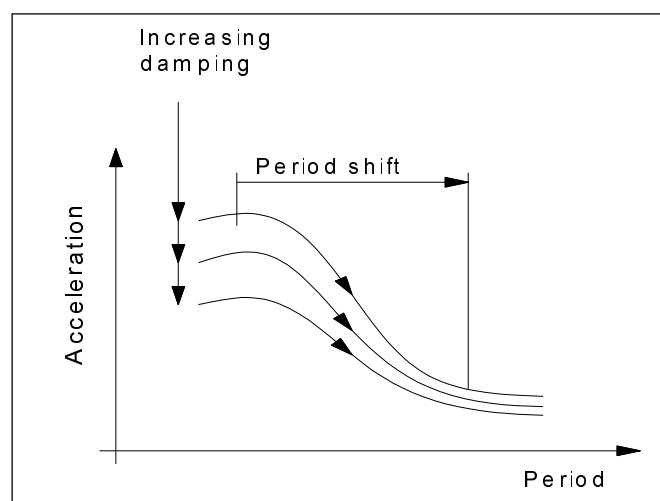


Figure 1.1 Acceleration response spectrum [2]

In Figure 1.1, note the rapid decrease in the acceleration transmitted to the isolated structure as the isolated period increases. This effect is equivalent to a rigid body motion of the building above the isolation level. The displacement of the isolator is controlled (to 100-400 mm) by the addition of an appropriate amount of damping (usually 5-20 % of critical). The damping is usually hysteretic, provided by plastic deformation of either steel shims or lead or ‘viscous’ damping of high-damping rubber. For these isolators strain amplitudes, in shear, often exceed 100%. The high damping has the effect of reducing the displacement by a factor of up to five from unmanageable values of ~1.0 m to large but reasonable sizes of <300 mm [22]. High damping may also reduce the cost of isolation since the displacements must be accommodated by the isolator components and the seismic gap, and also by flexible connections for external services such as water, sewage, gas and electricity.

The effect of damping for controlling displacement is shown in Figures 1.1 and 1.2, with increased damping reducing both the displacement of, and the accelerations to, the structure. But damping higher than 0.20 should be avoided since high isolator damping may seriously distort mode shapes, and complicate the analysis. In addition, higher mode responses increase as the damping increases. As a result of this substantial contribution of higher modes, seismic inertia forces increase when compared with those produced by only the first mode.

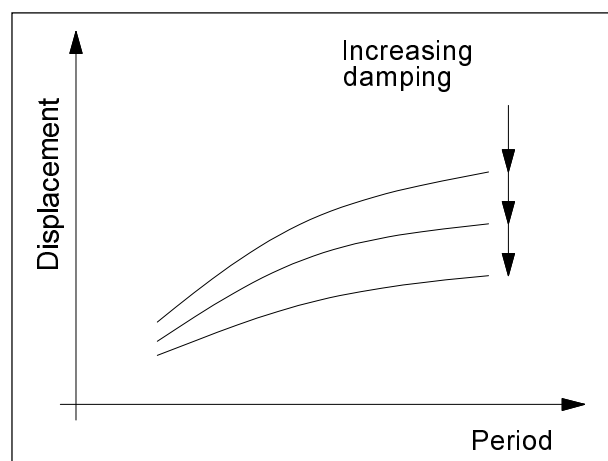


Figure 1.2 Displacement response spectrum [2]

1.2 Seismic Isolation Systems

The successful seismic isolation of a particular structure is strongly dependent on the appropriate choice of the isolator devices, or system, used to provide adequate horizontal flexibility with at least minimal centering forces and appropriate damping. It is also necessary to provide an adequate seismic gap that can accommodate all intended isolator displacements.

Most systems used today incorporate either elastomeric bearings, with the elastomer being either natural rubber or neoprene, or sliding bearings, with the sliding surface being Teflon and stainless steel although other sliding surfaces have been used. Systems that combine elastomeric bearings and sliding bearings have also been proposed and implemented [3].

1.2.1 Elastomeric Bearings

These bearings are fully developed commercial products whose main application have been for bridge superstructures, which often undergo substantial dimensional and shape changes due to changes in temperature. More recently their use has been extended to the seismic isolation of buildings and other structures. Elastomeric, non-lead-rubber bearings are available as either low-damping natural rubber bearing or high-damping bearings.

1.2.1.1 Low Damping Natural and Synthetic Rubber Bearings

Low-damping natural rubber bearings and synthetic rubber bearings are used in conjunction with supplementary damping devices, such as viscous dampers, steel bars, frictional devices, and so on. The elastomer used in bearings may be natural rubber or neoprene. The isolators have two thick steel endplates and many thin steel

shims. The rubber bearing consists of layer of rubber 5-20 mm thick, vulcanized between steel shims. The rubber layers give the bearing it's relatively low shear stiffness in the horizontal plane while the steel plates control the vertical stiffness and also determine the maximum vertical load, which can be applied safely. The steel plates also prevent the bulging of the rubber [1].

The material behavior in shear is quite linear up to shear strains above 100%, with the damping range of 2-3% of critical. The material is not subject to creep, and long-term stability of the modulus is good [5].

Low-damping elastomeric laminated bearings are simple to manufacture (the compounding and bonding processes to steel is well understood), easy to model, and their mechanical response is unaffected by rate, temperature, history, or aging. However in the structures they must be used with supplementary damping systems. These supplementary systems require elaborate connections and, in the case of metallic dampers, are prone to low-cycle fatigue [1].

1.2.1.2 High Damping Natural Rubber Bearings

The energy dissipation in high-damping rubber bearings is achieved by special compounding of the elastomer. Damping ratios will generally range between 8% and 20% of critical. The shear modulus of high-damping elastomers generally ranges between 0.34 MPa and 1.40 MPa. The material is nonlinear at shear strains less than 20% and characterized by higher stiffness and damping, which minimizes the response under wind load and low-level seismic load. Over the range of 20-120% shear strain, the modulus is low and constant. At large shear strains, the modulus and energy dissipation increase. This increase in stiffness and damping at large strains can be exploited to produce a system that is stiff for small input, is fairly linear and flexible at design level input, and can limit displacements under unanticipated input levels that exceed design levels [1].

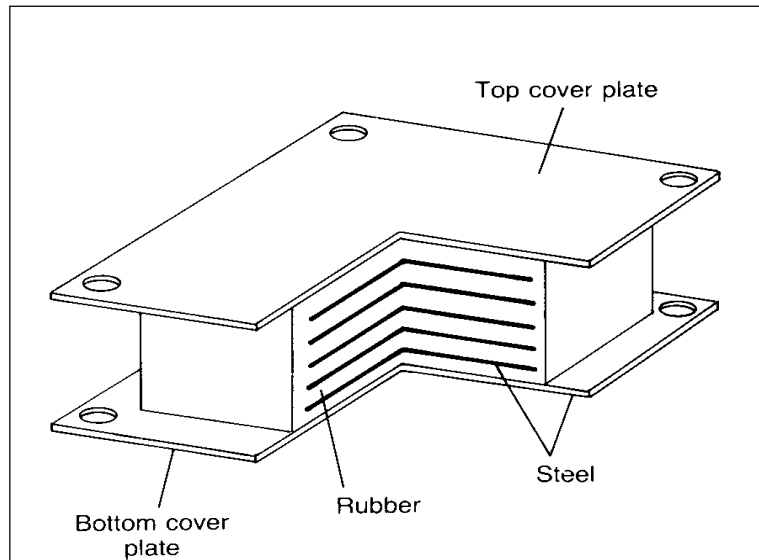


Figure 1.3 High damping rubber bearing [25]

1.2.1.3 Lead-Plug Bearings

Lead-plug bearings are generally constructed with low-damping elastomers and lead cores with diameters ranging 15% to 33% of the bonded diameter of the bearing. Laminated-rubber bearings are able to supply the required displacements for seismic isolation [1]. By combining them with a lead-plug insert which provides hysteretic energy dissipation, the damping required for a successful seismic isolation system can be incorporated in a single compact component. Thus one device is able to support the structure vertically, to provide the horizontal flexibility together with the restoring force, and to provide the required hysteretic damping.

The maximum shear strain range for lead-plug bearings varies as a function of manufacturer but is generally between 125% and 200%.

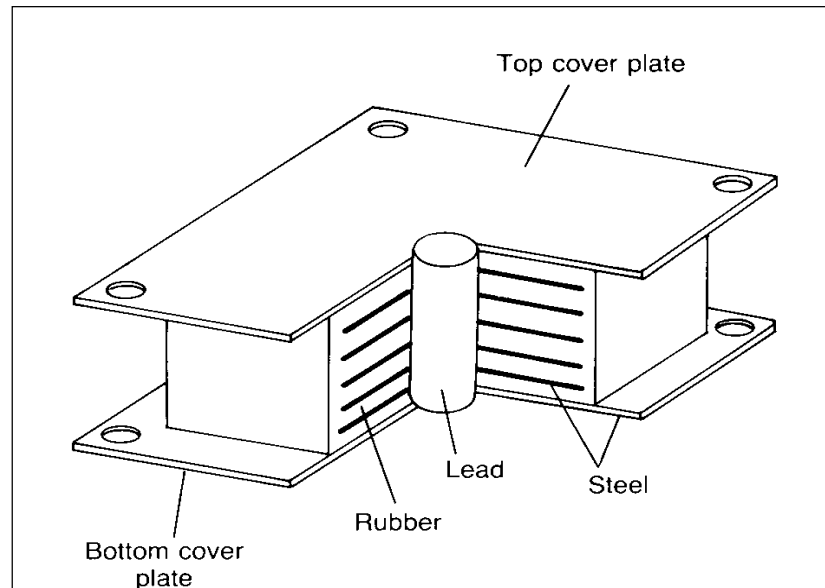


Figure 1.4 Lead-Plug bearing [25]

1.2.2 Isolation Systems Based on Sliding

One of the most popular and effective techniques for seismic isolation is through the use of sliding isolation devices. The sliding systems perform very well under a variety of severe earthquake loading and are very effective in reducing the large levels of the superstructure's acceleration. These isolators are characterized by insensitivity to the frequency content of earthquake excitation. This is due to tendency of sliding system to reduce and spread the earthquake energy over a wide range of frequencies. The sliding isolation systems have found application in both buildings and bridges. The advantages of sliding isolation systems as compared to conventional rubber bearings are:

- (i) Frictional base isolation system is effective for a wide range of frequency input,
- (ii) Since the frictional force is developed at the base, it is proportional to the mass of the structure and the center of mass and center of resistance of the

sliding support coincides. Consequently, the torsional effects produced by the asymmetric building are diminished.

1.2.2.1 Pure-Friction System

The simplest sliding isolation system is the pure friction system. In this system a sliding joint separates the superstructure and the substructure. The use of layer of sand or roller in the foundation of the building is the example of pure-friction base isolator. The pure-friction type base isolator is essentially based on the mechanism of sliding friction. The horizontal frictional force offers resistance to motion and dissipates energy. Under normal conditions of ambient vibrations and small magnitude earthquakes, the system acts like a fixed base system due to the static frictional force. For large earthquake the static value of frictional force is overcome and sliding occurs thereby reducing the accelerations.

1.2.2.2 Resilient-Friction Base Isolation System

Mostaghel and Khodaverdian (1987) proposed the resilient-friction base isolation (R-FBI) system as shown in Figure 1.5. This base isolator consists of concentric layers of Teflon-coated plates that are in friction contact with each other and contains a central core of rubber. It combines the beneficial effect of friction damping with that of resiliency of rubber. The rubber core distributes the sliding displacement and velocity along the height of the R-FBI bearing. They do not carry any vertical loads and are vulcanized to the sliding ring. The system provides isolation through the parallel action of friction, damping and restoring force [1].

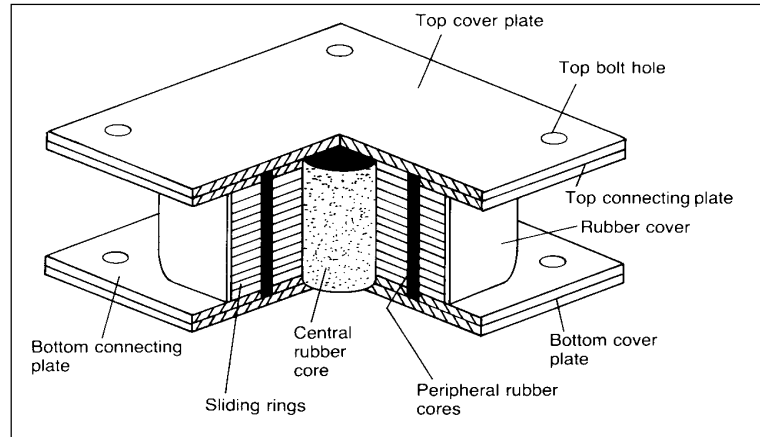


Figure 1.5 Resilient-friction base isolation system [25]

1.2.2.3 Electric de France System

An important friction type base isolator is a system developed under the auspices of “Electric de France” (EDF) (Gueraud et. al., 1985). This system is standardized for nuclear power plants in region of high seismicity. The base raft of the power plant is supported by the isolators that are in turn supported by a foundation raft built directly on the ground. The main isolator of the EDF consists of laminated (steel reinforced) neoprene pad topped by lead-bronze plate that is in friction contact with steel plate anchored to the base raft of the structure. The friction surfaces are designed to have a coefficient of friction of 0.2 during the service life of the base isolation system.

The EDF base isolator essentially uses elastomeric bearing and friction plate in series. An attractive feature of EDF isolator is that for lower amplitude ground excitation the lateral flexibility of neoprene pad provides base isolation and at high level of excitation sliding will occur which provides additional protection. This dual isolation technique was intended for small earthquakes where the deformations are concentrated only in the bearings. However, for larger earthquakes the bronze and steel plates are used to slide and dissipate seismic energy. The slip plates have been designed with a friction coefficient equal to 0.2 and to maintain this for the life time of the plant [1].

1.2.2.4 Friction Pendulum System

The concept of sliding bearings is also combined with the concept of a pendulum type response, obtaining a conceptually interesting seismic isolation system known as a friction pendulum system (FPS) (Zayas et al., 1990) as shown in Figure 1.6. In FPS, the isolation is achieved by means of an articulated slider on spherical, concave chrome surface. The slider is faced with a bearing material which when in contact with the polished chrome surface, results in a maximum sliding friction coefficient of the order of 0.1 or less at high velocity of sliding and a minimum friction coefficient of the order of 0.05 or less for very low velocities of sliding. The dependency of coefficient of friction on velocity is a characteristic of Teflon-type materials (Mokha et al., 1990). The system acts like a fuse that is activated only when the earthquake forces overcome the static value of friction. Once set in motion, the bearing develops a lateral force equal to the combination of the mobilised frictional force and the restoring force that develops as a result of the induced rising of the structure along the spherical surface. If the friction is neglected, the equation of motion of the system is similar to the equation of motion of a pendulum, with equal mass and length equal to the radius of curvature of the spherical surface. The seismic isolation is achieved by shifting the natural period of the structure. The natural period is controlled by selection of the radius of curvature of the concave surface. The enclosing cylinder of the isolator provides a lateral displacement restraint and protects the interior components from environmental contamination. The displacement restraint provided by the cylinder provides a safety measure in case of lateral forces exceeding the design values [1].

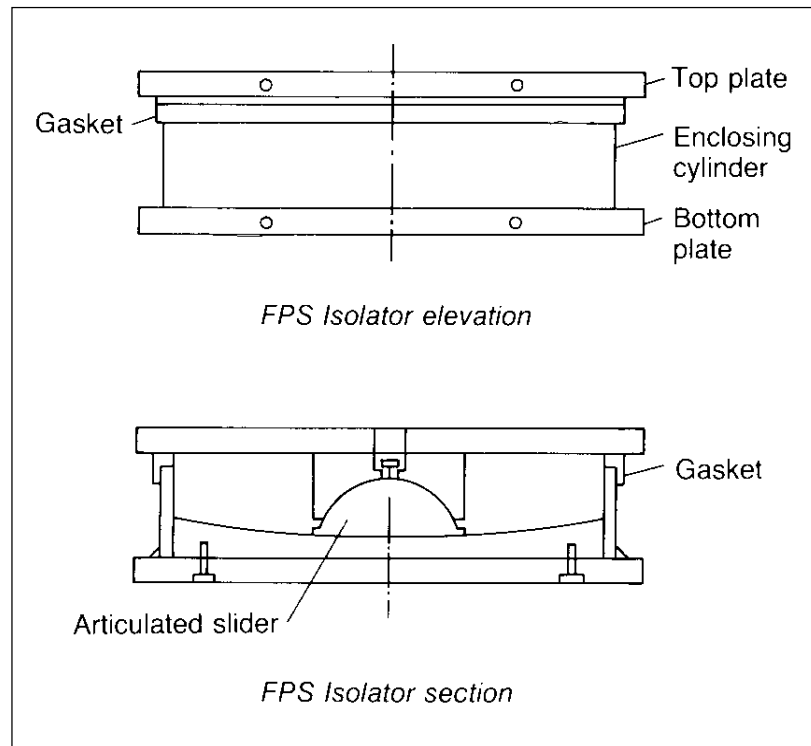


Figure 1.6 Friction pendulum system [25]

1.3 Current Applications

The seismically isolated buildings fall into two broad categories: fragile structures of historic significance and new structures with contents, which need to be protected or continue to operate during and immediately after the earthquake. It is seen that most base isolated buildings around the world are important buildings such as hospitals, universities, schools, firehouses, nuclear power plants, municipal and governmental buildings, and some high technology buildings that house sensitive internal equipment or machinery.

There are many examples of base-isolated structures in the United States and Japan. A number of base-isolated buildings have been built in New Zealand and in Italy. Demonstration projects that apply low-cost base isolation systems for public housing

in developing countries have been completed in Chile, the People's Republic of China, Indonesia, and Armenia [4].

In the United States the most commonly used isolation system is the lead-plug rubber bearing. Although some projects are isolated solely with lead-plug bearings, they are generally used in combination with multilayered elastomeric bearings without lead plugs.

Many isolation systems used in Japan and New Zealand combine low-damping natural rubber bearings with some form of mechanical damper. This includes hydraulic dampers, steel bars, steel coils, or lead plugs within the building itself. There are several drawbacks to using dampers for isolating structures: Every type of damper –except the internal lead plug- requires mechanical connectors and routine maintenance, the yielding of metallic dampers introduces a nonlinearity into the response that complicates the analysis of the dynamic response of the isolated building, and they reduce the degree of isolation by causing response in higher modes [2].

In Turkey, especially in some of the prestigious projects the application of seismic isolation technique has started to be used in recent years. For example, the new \$300 million International Terminal at Istanbul's Atatürk Airport is a massive, two hundred and fifty thousand square meters building that serves as the port of entry for 14 million international air passengers to Turkey each year. The main feature of the terminal is the 250m by 225m pyramidal roof space frame with triangular skylights. This delicate roof structure is supported by 130 Friction Pendulum bearings, placed between the roof frame and the concrete columns that rise 7m above the departure level. The bearings protect the delicate roof glass, glass curtain walls, and the cantilever columns in the event of a major earthquake. Some of the important isolated buildings are listed in Table 1.1.

Table 1.1 Current applications of seismic isolation [4]

No	Buildings	Year	City	Size	Description
1	Foothill Law and Justice Center, San Bernardino	1985	Los Angeles, USA	15800 m ² N = 4	21 km distance to the fault, 98 bearings, \$38 million high damping natural rubber.
2	Fire Command and Control Facility	1997	Los Angeles, USA	5000 m ² N = 2	High damping natural rubber 6% less cost than conventional design.
3	Emergency Operations Center	1998	Los Angeles, USA	8000 m ² N = 3	28 high damping natural rubber bearings
4	Traffic Management Center for Caltrans, Kearny Mesa	1997	San Diego, USA	N = 2	40 bearings t= 60 cm T _D = 2,5 sec., d _D = 25 cm
5	M.L. King / C.R. Drew Diagnostics Trauma Center	1995	Willowbrook Los Angeles, USA	13000 m ² N = 5	70 high damping rubber bearings, 12 sliding pad D=100cm
6	Flight Simulator Manufacturing Facility	1998	Salt Lake City, USA	10800 m ² N = 4	50 pads 46cm / 48 pads 38cm T _D = 2,5 sec., d _D = 23 cm
7	Auto Zone Office Building	1997	Memphis, USA	23230 m ² N = 8	43 rubber isolators \$27 million
8	International Terminal, San Francisco Airport	1999	San Francisco, USA	28000m ²	Friction Pendulum Isolators
9	Hayward City Hall, CA	1999	Hayward, USA	14000m ²	Friction Pendulum Isolators
10	West Japan Postal Computer Center, Sanda	1986	Sanda, Japan	47000 m ² N = 6	120 elastomeric pads, T _D =3,9 sec.
11	Matsumura-Gumi Technical Research Institute	1989	Japan	12000 m ² N = 8	High damping natural rubber bearings
12	Administration Center, National Telephone Company	1998	Ancona, Italy	5 buildings 12000 m ² N=7	High damping rubber bearings

Table 1.1 (continued)

No	Buildings	Year	City	Size	Description
13	Residential Apartment Building, Squillace	1999	Calabria, Italy	2600 m ² N = 4	High damping rubber bearings
14	Administrative Building, Ministry of Defense	2000	Ancona, Italy	6800 m ² N = 4	High damping rubber bearings
15	William Clayton Building, Wellington	1981	New Zealand	-	Lead-Rubber bearings
16	Union House, Auckland	1988	New Zealand	13600 m ² N = 13	Lead-Rubber bearings
17	Central Police Station, Wellington	1989	New Zealand	12400 m ² N = 10	Lead-extension dampers
18	National Museum, Wellington	1997	New Zealand	22000 m ² N = 6	142 lead-rubber bearings 36 teflon pads
19	Printing Press Building, Peton, Wellington	1990	New Zealand	16000 m ² N = 4	Lead-Rubber bearings

1.4 Literature Survey

The codes and guidelines for design of structures with seismic base isolation have evolved from the design provisions that were developed in the 1980s by a subcommittee of the Structural Engineers Association of Northern California (SEAONC). In 1986 SEAONC published a simple regulation titled “Tentative Seismic Isolation Design Requirements”, also known as the Yellow Book [1]. The Yellow Book, mainly based on equivalent static design methods, implemented in the various editions of the Uniform Building Code (UBC) [9], the most widely used code for design of earthquake resistant buildings in the United States. The Yellow Book modified and became the 1991 version of the UBC, “Earthquake Regulations for Seismic-Isolated Structures”. The 1994 and 1997 versions of UBC are elaborated. As

the UBC-97 has evolved, International Building Code 2000 [11] (IBC2000) has become extremely complex code based mainly on dynamic methods of design.

The seismic upgrade design of existing structures is influenced by the National Earthquake Hazards Reduction Program (NEHRP) Guidelines for the Seismic Rehabilitation of Buildings, FEMA-273 [17], and its commentary FEMA-356 [16], which are published by the Federal Emergency Management Agency. The FEMA-273 provisions are very similar to those of the IBC2000 with one basic exception: FEMA-273 permits pushover method.

In addition to the design codes, various textbooks are available providing complete, up to date coverage of seismic isolation concept.

In their exceptional textbook, Naeim and Kelly [1] present detailed information about current seismic isolation components. [1] serves as a guide to understand isolation concept, procedures involved in design of seismic isolated structures, and complex code requirements. UBC-97 is used for numerical examples and evaluated in details. Where appropriate, UBC-97 requirements are compared and contrast with those of FEMA-273 and other important documents. Furthermore, an overview of available computer programs for analysis of seismic isolated structures and using the SAP2000 nonlinear program to model nonlinear isolation systems are presented.

The more advanced textbook on seismic isolation is the one of Skinner, Robinson and McVerry [2]. It explores the theoretical concepts in more detail. [2] mainly concentrates on the mathematical analysis of the seismic responses of isolated structures, discussion of isolation systems and guidelines to provide initial isolator parameter values for engineers wishing to incorporate seismic isolation into their designs.

In [4], Tezcan and Cimilli suggest a complete formulation similar to that of UBC-1997 for use in a possible future version of the Turkish seismic code for designing structures with seismic base isolation. It is advocated that the formulation supplied in

the Turkish seismic code [8], for the calculation of the lateral earthquake loads, can be adjusted for the design of base isolated structures.

Matsagar and Jangid [20], in their noteworthy paper, present a study about the influence of isolator characteristic parameters on the response of multi-story base isolated structures. The effects of the shape of isolator loop and superstructure flexibility on the seismic response is investigated.

1.5 Aims and Scope

The aim of this study is to investigate the effects of seismic base isolation systems, especially rubber bearings, on the response of structures. The study includes analysis of the seismic responses of isolated structures, which is oriented to give a clear understanding of the processes involved and discussion of various isolators.

The notes introduce the related chapters of FEMA and IBC2000 regulations for the seismic isolated structures. These provisions and formulas, their similarities and differences, are presented. Case studies illustrate their use in both static and dynamic analyses. The static equivalent lateral force of analysis, response spectrum analysis and time history analysis are carried out in case studies. Design procedures used for base isolated systems are discussed and form the basis for preliminary design procedures. Using a consistent set of design criteria, a commercial computer program SAP2000 demonstrates the ease with which the design for isolated systems may be executed.

No specific provisions are included in the Turkish seismic code (ABYYHY-98) [8] for the earthquake resistant design of buildings with seismic base isolation. Therefore the seismic base isolation provisions of the FEMA [17] and IBC2000 [11] have been utilized in the design examples. Nevertheless, the discussion of the case study results is done by considering the Turkish seismic code and some important conclusions for use in possible future version of the Turkish seismic code are drawn.

CHAPTER 2

MATHEMATICAL MODELLING OF ISOLATORS

Seismic isolation bearings are generally characterized as either linear viscoelastic components or bilinear components. In practice all isolation bearings can be modeled by bilinear models where as high-damping rubber bearings are generally modeled as linear elastic-viscous models. For more detail explanation, one may refer to [20].

2.1 Mechanical Characteristics of Elastomeric Isolators

The horizontal stiffness of a bearing is given by [1]:

$$K_H = \frac{(GA)}{t_r} \quad (2.1)$$

where G is the shear modulus of the elastomer, A is the total cross-sectional area, and t_r is the total thickness of the rubber only. Another design characteristic of an isolator is the vertical stiffness K_V which is the dominant parameter controlling the vertical frequency of an isolated structure. The vertical stiffness of a rubber bearing is given by the formula [1]:

$$K_V = \frac{(E_c A)}{t_r} \quad (2.2)$$

where E_c is the instantaneous compression modulus of the rubber-steel composite under the specified level of vertical load.

2.1.1 Comparison of Compression Modulus

The compression modulus of a circular bearing (E_c) is defined by different formulas in FEMA-356 [16] and Naeim and Kelly study [1].

$$E_c = \left(\frac{1}{6GS^2} + \frac{4}{3K} \right)^{-1} \quad [\text{FEMA-356}] \quad (2.3)$$

$$E_c = \left(\frac{1}{6GS^2} + \frac{1}{K} \right)^{-1} \quad [\text{Naeim and Kelly}] \quad (2.4)$$

E_c	→	Compression Modulus	
S	→	Shape Factor	($5 < S < 30$)
K	→	Bulk Modulus	($1000\text{MPa} < K < 2500 \text{MPa}$)
G	→	Shear Modulus	($0.5\text{MPa} < G < 2.5 \text{MPa}$)

Figures 2.1 – 2.3 are prepared in order to demonstrate how the compression modulus of a circular pad changes according to these two different formulas for given intervals of shape factor (S), bulk modulus (K), and shear modulus (G).

E_c – S Relationship

To be able to evaluate the effect of shape factor (S) only, shear modulus (G) and bulk modulus (K) are taken as constant, 1.0 MPa and 2000 MPa, respectively. By examining Figure 2.1, it can be said that the two formulas give very close results up to $S = 12$. Thus, they can be assumed as identical for $5 < S < 12$ interval. On the other hand, for the “ S ” vales greater than 12 the outcomes of the formulas show

considerable difference and this difference increases as the “S” value increases. The formula given by Naeim and Kelly gives greater compression modulus values when compared to the formula given in FEMA for $12 \leq S < 25$ interval.

E_c – G Relationship

Shape factor (S) and bulk modulus (K) are taken as 15 and 2000 MPa respectively, in order to demonstrate the effect of shear modulus (G) in Figure 2.2. It is obvious from the figure that the calculated “ E_c ” values from the formulas show considerable difference and this difference increases as the “G” value increases. The formula given by Naeim and Kelly gives greater compression modulus values when compared to the formula given in FEMA for $0.5 \text{ MPa} < G < 2.5 \text{ MPa}$ interval.

E_c – K Relationship

In Figure 2.3 shape factor (S) and shear modulus (G) are taken as 15 and 1.0 MPa respectively, in order to demonstrate the effect of bulk modulus (K). It is obvious from the figure that the formula given by Naeim and Kelly gives greater compression modulus values when compared to the formula given in FEMA. The calculated “ E_c ” values from the two formulas show a constant difference in the range of 100 MPa no matter what the value of “K” is.

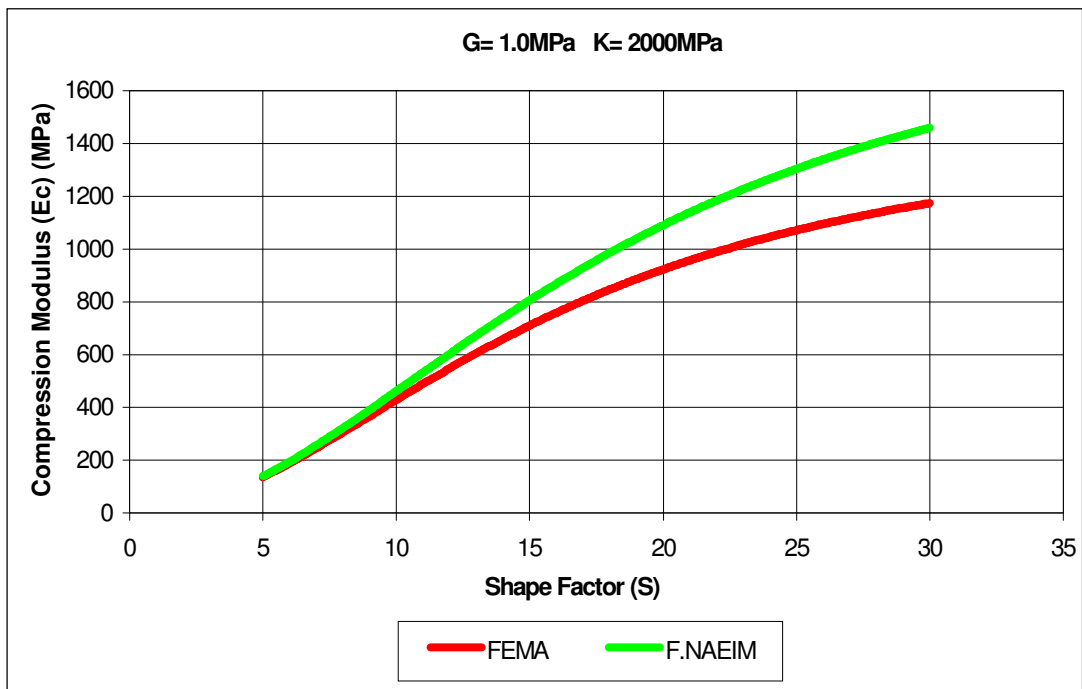


Figure 2.1 $E_c - S$ relationship

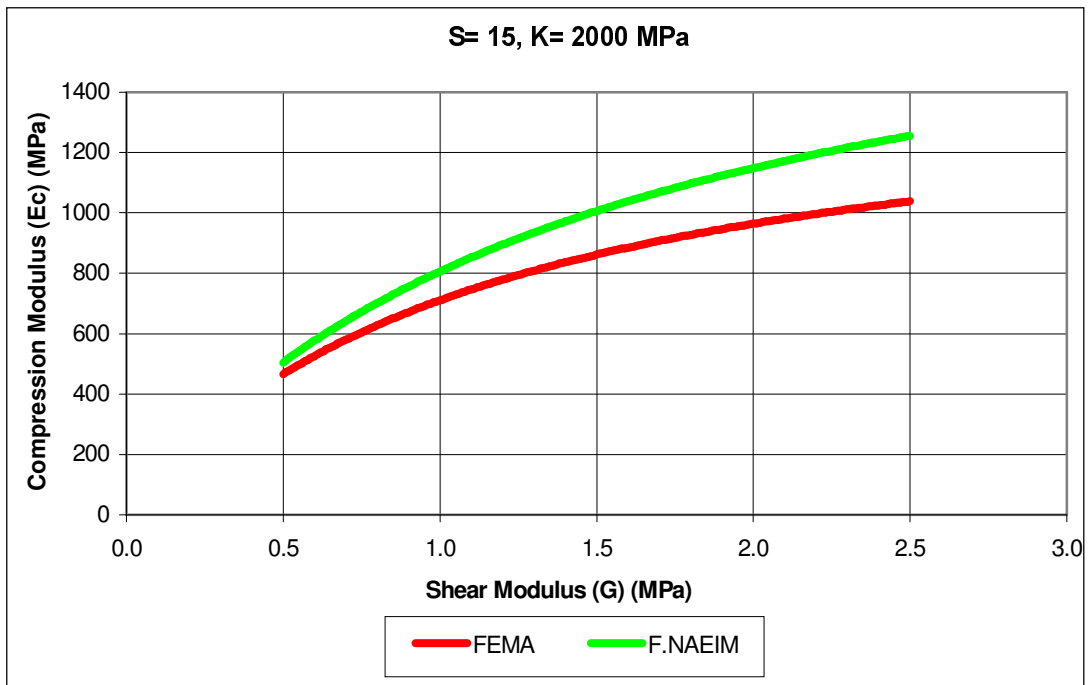


Figure 2.2 $E_c - G$ relationship

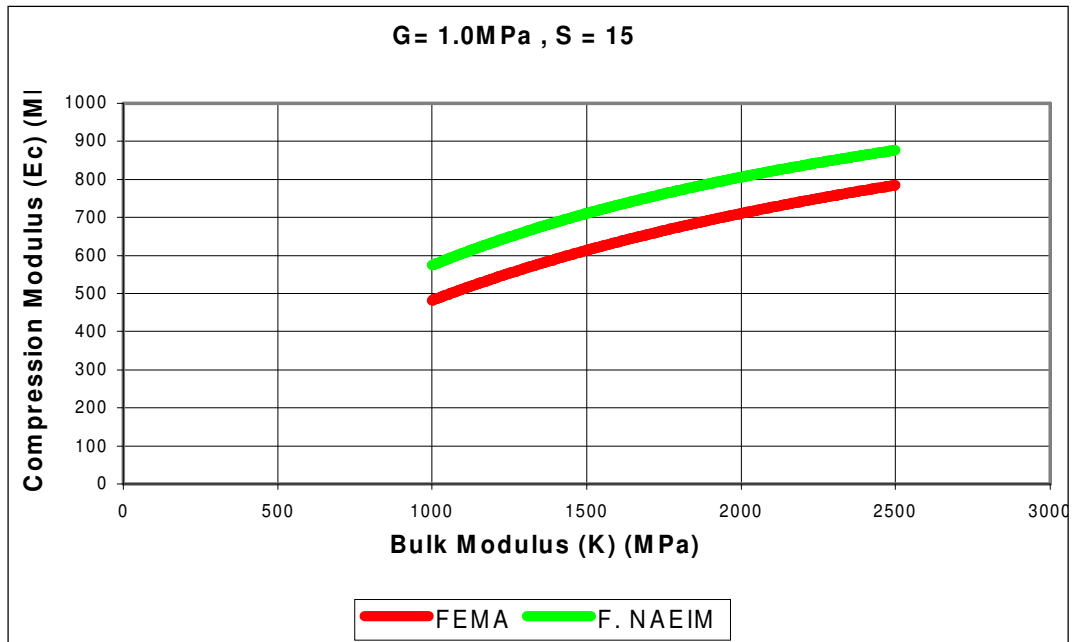


Figure 2.3 $E_c - K$ relationship

The comparison of Figures 2.1–2.3 shows that Naeim and Kelly gives higher compression modulus compared to FEMA for the same pad. Consequently, bearings are assumed to be stiffer in vertical direction when compared to FEMA.

2.2 Equivalent Linear Model of Isolators

The non-linear force-deformation characteristic of the isolator can be replaced by an equivalent linear model through effective elastic stiffness and effective viscous damping. The equivalent linear elastic stiffness for each cycle of loading is calculated from experimentally obtained force-deformation curve of the isolator and expressed mathematically as [11]:

$$k_{eff} = \frac{(F^+ - F^-)}{(\Delta^+ - \Delta^-)} \quad (2.5)$$

where F^+ and F^- are the positive and negative forces at test displacements Δ^+ and Δ^- , respectively. Thus, the k_{eff} is the slope of the peak-to-peak values of the hysteresis loop as shown in Figure 2.4.

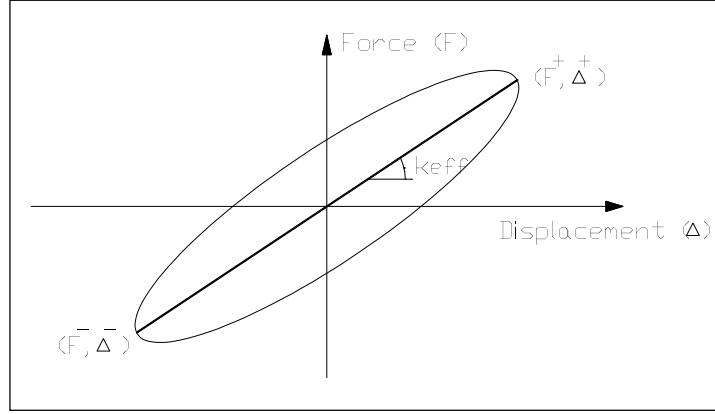


Figure 2.4 Force displacement relationship of equivalent linear model [20]

The effective viscous damping ratio of the isolator calculated for each cycle of loading is expressed as [11]:

$$\beta_{eff} = \frac{(2E_{loop})}{[\pi k_{eff} (|\Delta^+| - |\Delta^-|)^2]} \quad (2.6)$$

where E_{loop} is the energy dissipation per cycle of loading.

2.3 Bilinear Model of Isolators

Bilinear model can be used for all isolation systems used in practice. In fact only bilinear hysteretic model can reflect the non-linear characteristics of the lead-plug bearings and friction-pendulum systems that are commonly used isolation systems. The non-linear force-deformation behavior of the isolation system is modeled through the bilinear hysteresis loop based on the three parameters (i) elastic stiffness,

K_1 (ii) post-yield stiffness, K_2 (iii) characteristic strength, Q (Figure 2.5). The characteristic strength, Q is related to the yield strength of the lead plug inserted in the elastomeric bearing or friction coefficient of the sliding type isolation system [20].

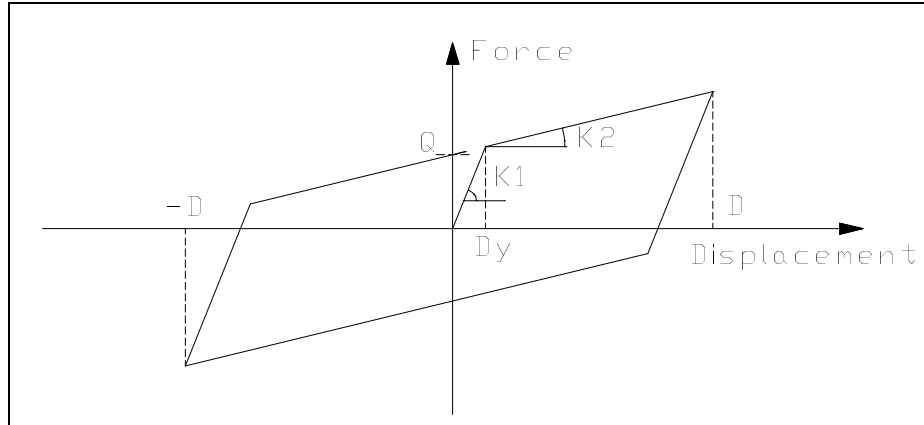


Figure 2.5 Force displacement relationship of bilinear model [1]

At specified design displacement, D , the effective stiffness for a bilinear system is expressed as [1]:

$$k_{eff} = K_2 + \left(\frac{Q}{D}\right) \quad D > D_y \quad (2.7)$$

where D_y is the yield displacement. In terms of the primary parameters [1]:

$$D_y = \frac{Q}{(K_1 - K_2)} \quad (2.8)$$

The effective damping β_{eff} is expressed as [1]:

$$\beta_{eff} = \frac{4Q(D - D_y)}{(2\pi k_{eff} D^2)} \quad (2.9)$$

2.4 Comparison of Response for Bilinear and Equivalent Linear Model

To investigate and compare the differences in the seismic responses of buildings isolated by bilinear and equivalent linear isolator models, a five-story symmetrical building, introduced in Section 3.2.2, is chosen. Two different types of isolators, lead-plug bearings (LPB) and friction pendulum system (FPS), are used for bilinear modeling where as type of the isolator is not important for equivalent linear modeling. The nonlinear time history method is used for the analyses by the help of a commercial computer program SAP2000. The earthquake motions selected for the study are S50W component of 1979 Imperial Valley earthquake (IMPERIAL), EW component of 1999 Kocaeli earthquake (KOCAELI), HORIZ0 component of 1989 Loma Prieta earthquake (LOMA). The peak ground acceleration (PGA) of Imperial Valley, Kocaeli and Loma Prieta earthquake motions are 0.46g, 0.23g and 0.63g, respectively. The acceleration and displacement spectra of the ground motions for 2% damping are shown in Figures 2.6 and 2.7. The damping ratio is selected as 2% for the spectra because the damping ratio of the superstructure, β_s , is taken as 0.02 for the analyses.

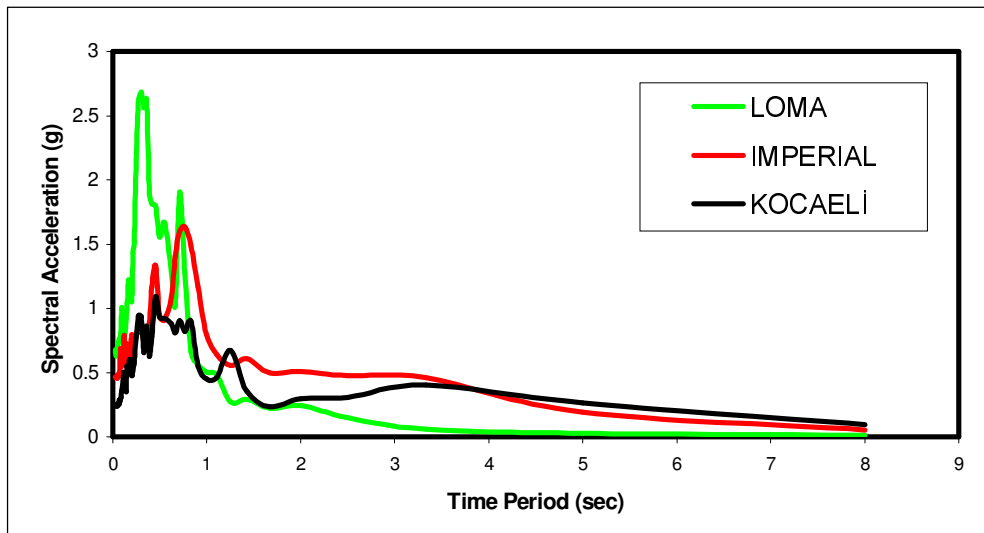


Figure 2.6 Acceleration spectra

The investigated response quantities are the top floor acceleration and bearing displacement. These response quantities are important because floor accelerations

developed in the structure are proportional to the forces exerted as a result of an earthquake ground motion. On the other hand, the bearing displacements are crucial in the design of isolation systems.

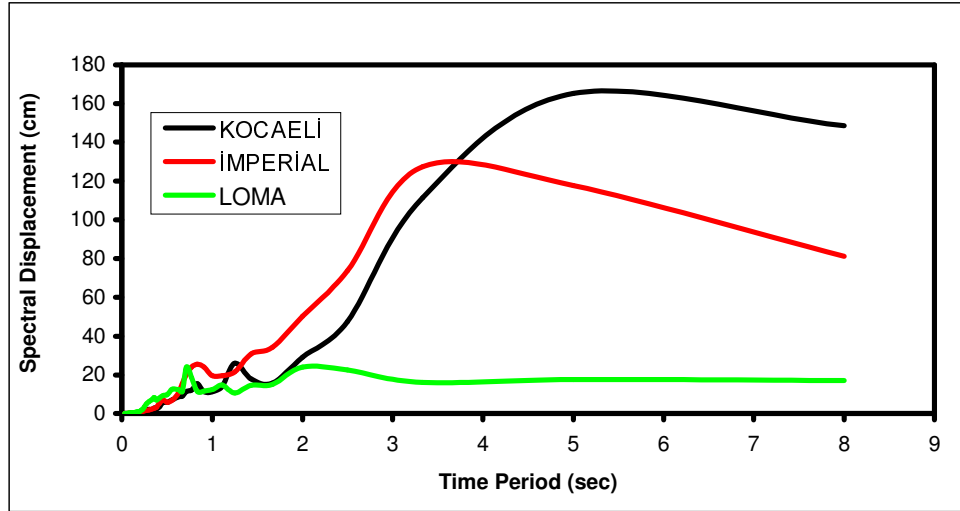


Figure 2.7 Displacement spectra

The parameters for the bilinear model isolators are determined according to the parameters of equivalent linear model which are depended on the selected target period T and the effective viscous damping β_{eff} . In addition to the T and β_{eff} , the design displacement, D , is also necessary for the determination of the parameters of bilinear model. The design displacement, equal to the maximum isolator displacement, is calculated as a result of the analysis of the structure isolated by the equivalent linear model isolators having the parameters T and β_{eff} . For the assumed value of yield displacement, D_y , depending upon the selected type of bilinear isolation system, the parameters of bilinear hysteresis loop is determined such that it has a period as equal to T and damping ratio as β_{eff} by using Equations 2.7, 2.8 and 2.9 given above.

The values of design displacement, D , used for such transformation are 49.6, 29.6 and 24.9 cm under Imperial Valley, Kocaeli and Loma Prieta ground motions respectively, obtained from equivalent linear model analysis with $T=2.1$ sec.,

$k_{eff}=805$ kN/m and $\beta_{eff}=0.15$. When the design displacement values, D , of the three earthquakes are compared:

$$D_{(imperial\ valley)} > D_{(kocaeli)} > D_{(loma\ prieta)}$$

If the spectra given in Figures 2.6 and 2.7 are taken into account for $T = 2.1$ sec., this is an expected trend. Because according to the acceleration spectra and displacement spectra, while Imperial Valley earthquake gives the most critical results, Loma Prieta earthquake gives the least critical values when $T = 2.1$ sec.

Table 2.1 The parameters of bilinear hysteresis loop

	Imperial Valley		Kocaeli		Loma Prieta	
D (cm)	49.6		29.6		24.9	
D_y (mm)	2.5 (typical for FPS)	25 (typical for LPB)	2.5 (typical for FPS)	25 (typical for LPB)	2.5 (typical for FPS)	25 (typical for LPB)
Q (kN)	94.6	99.1	56.6	61.3	47.7	52.5
K₂ (kN/m)	614.4	605.3	613.7	597.8	613.4	594.2
K₁ (kN/m)	38438	4568	23253	3049	19689	2693

For the bilinear isolator models, two values of yield displacement, D_y , are taken into account as 2.5 mm and 25 mm which mostly correspond to friction pendulum system (FPS) and lead-plug bearing (LPB) isolators [1], respectively. The time variation of top floor acceleration and bearing displacement is given in Figures 2.8 and 2.9 under the effect of Imperial Valley earthquake for bilinear and linear isolator models. The peak top floor accelerations obtained by bilinear hysteretic model are 0.59g and 0.43g for the yield displacement of 2.5mm and 25mm respectively. The corresponding peak top floor acceleration obtained from equivalent linear model is 0.38g. This implies that the equivalent linear model as compared to bilinear hysteretic model underestimates the force exerted on superstructure by the ground motion.

On the other hand, the peak bearing displacement obtained by the bilinear hysteretic model is 22.9 and 26.2 cm for the yield displacements of 2.5 and 25 mm, respectively, whereas, that obtained from its equivalent linear model is 49.6 cm. This implies that the equivalent linear model when compared to bilinear hysteretic model overestimates the bearing displacement in an isolated structure. Similar results of equivalent linear model and bilinear hysteretic model is also observed for Kocaeli and Loma Prieta earthquake ground motions which are shown in Table 2.2.

Table 2.2 Results of the analyses

	Maximum Top Floor Acceleration			Maximum Bearing Displacement		
	Linear	Bilinear		Linear	Bilinear	
Typical FPS $D_y = 2.5$ mm		Typical LPB $D_y = 25$ mm	Typical FPS $D_y = 2.5$ mm		Typical LPB $D_y = 25$ mm	
Imperial Valley	0.38g	0.59g	0.43g	49.6 cm	22.9 cm	26.2 cm
Kocaeli	0.11g	0.32g	0.21g	29.6cm	9.2cm	14.0cm
Loma Prieta	0.09g	0.25g	0.18g	24.9cm	6.9cm	8.6cm

As a result, it can be concluded that the equivalent linear model underestimates the peak superstructure acceleration and overestimates the bearing displacement when compared to the actual bilinear hysteretic model.

In Figures 2.9, 2.11 and 2.13 time variation of bearing displacements are given under the effect of Imperial Valley Earthquake, Kocaeli Earthquake and Loma Prieta Earthquake, respectively. It is observed from the figures that a permanent displacement, which is a result of yielding in bearings, takes place for bilinear models. This outcome shows the necessity of installing a supplementary system producing re-centering force for the bearings.

In Figures 2.14, 2.15 and 2.16, force-deformation diagrams of bilinear models are given in order to understand the effect of isolator yield displacement on the response

of an isolated structure. It is observed that the bearing displacements show an increasing trend with the increase in the isolator yield displacement. For example; the peak bearing displacements for Kocaeli earthquake read from the Figure 2.15 are 9.2 cm and 14.0 cm for the yield displacement of 2.5mm and 25mm respectively. Since the same trend is also valid for the other ground motions, it can be concluded that with the increase in isolator yield displacement, D_y , the bearing displacement also increases. But the percentage of the increase depends on the effectiveness of the source type.

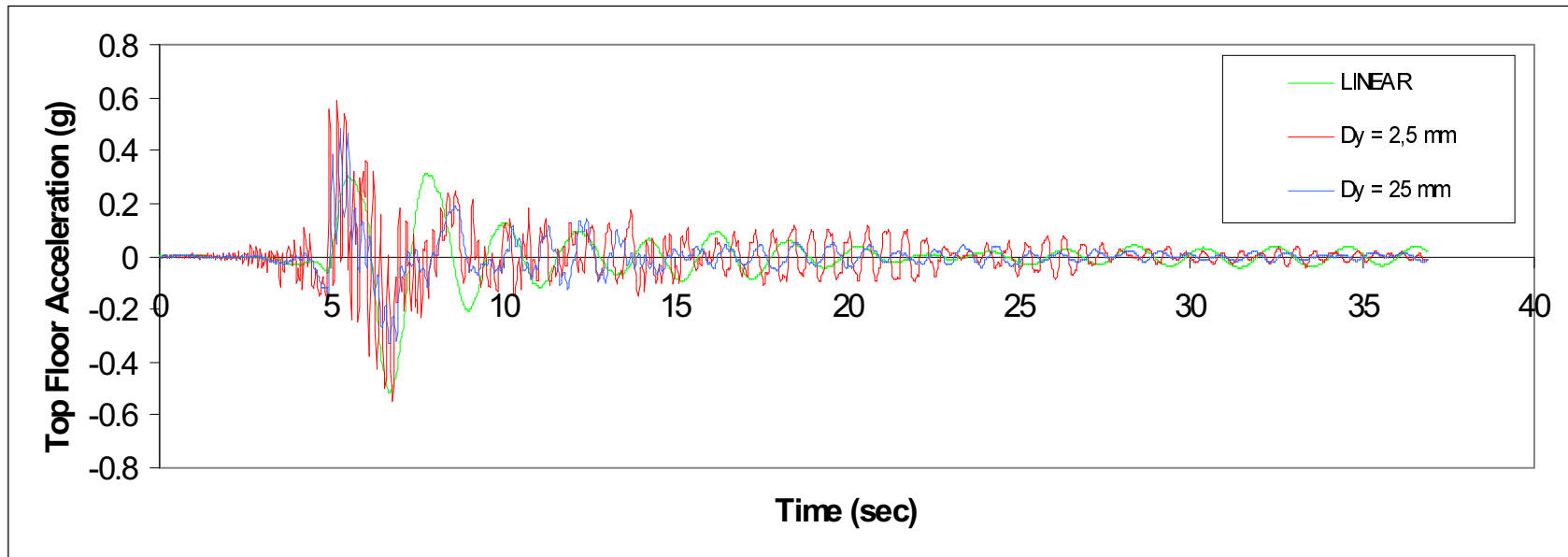


Figure 2.8 Time variation of top floor acceleration under the effect of Imperial Valley (1979) earthquake.

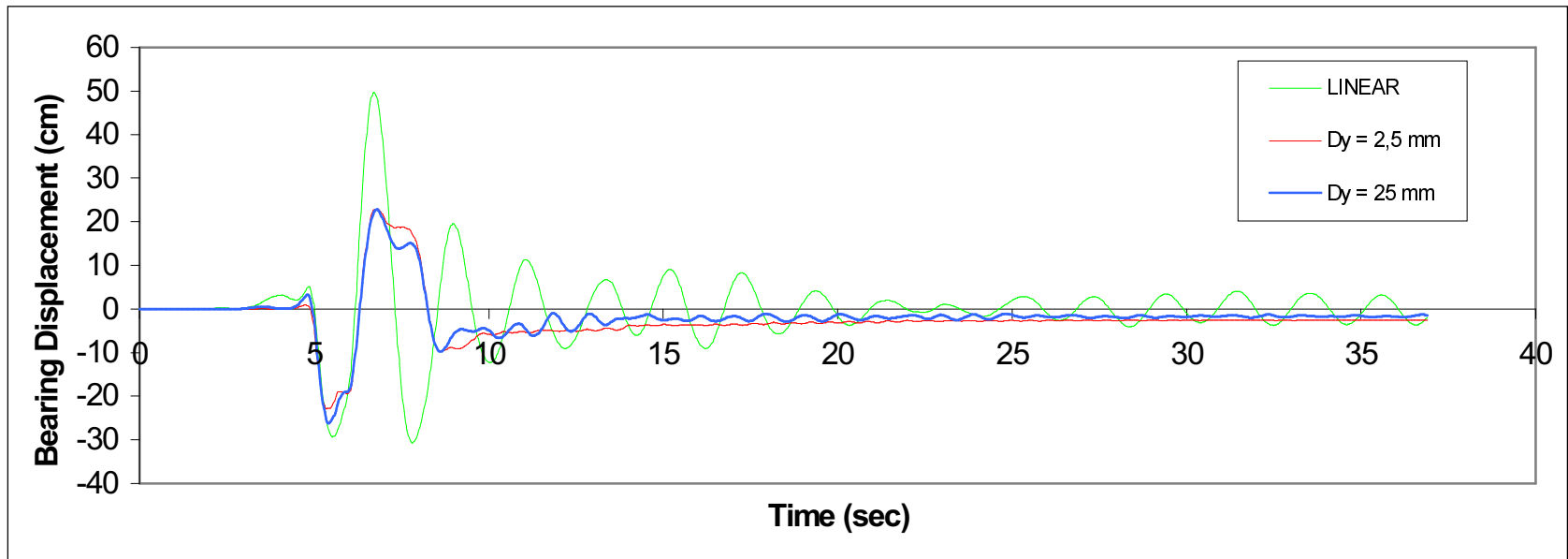


Figure 2.9 Time variation of bearing displacement under the effect of Imperial Valley (1979) earthquake.

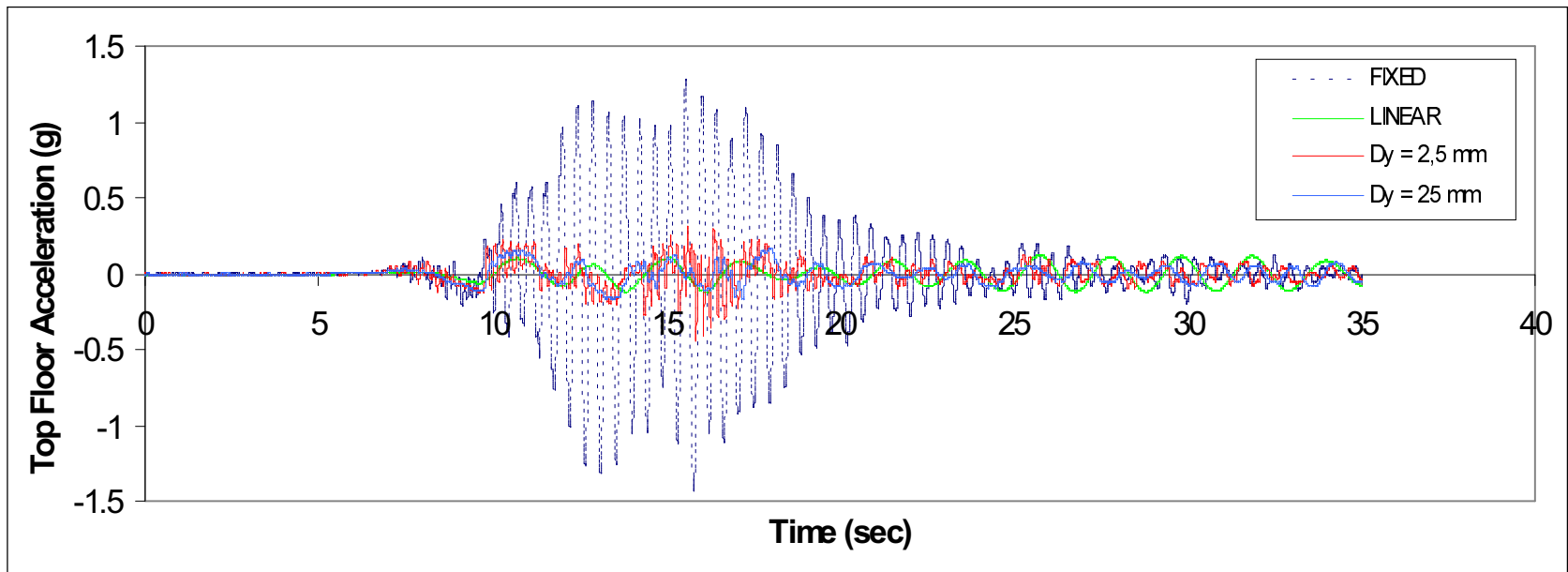


Figure 2.10 Time variation of top floor acceleration under the effect of Kocaeli (1999) earthquake.

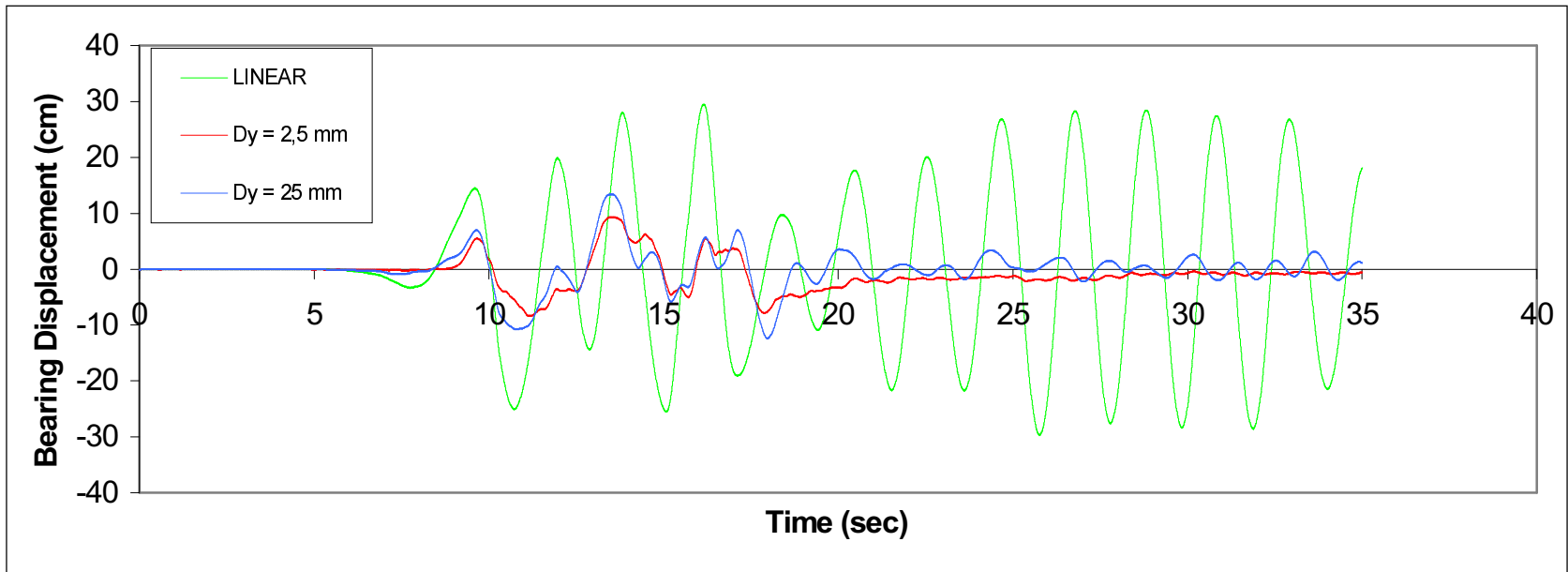


Figure 2.11 Time variation of bearing displacement under the effect of Kocaeli (1999) earthquake.

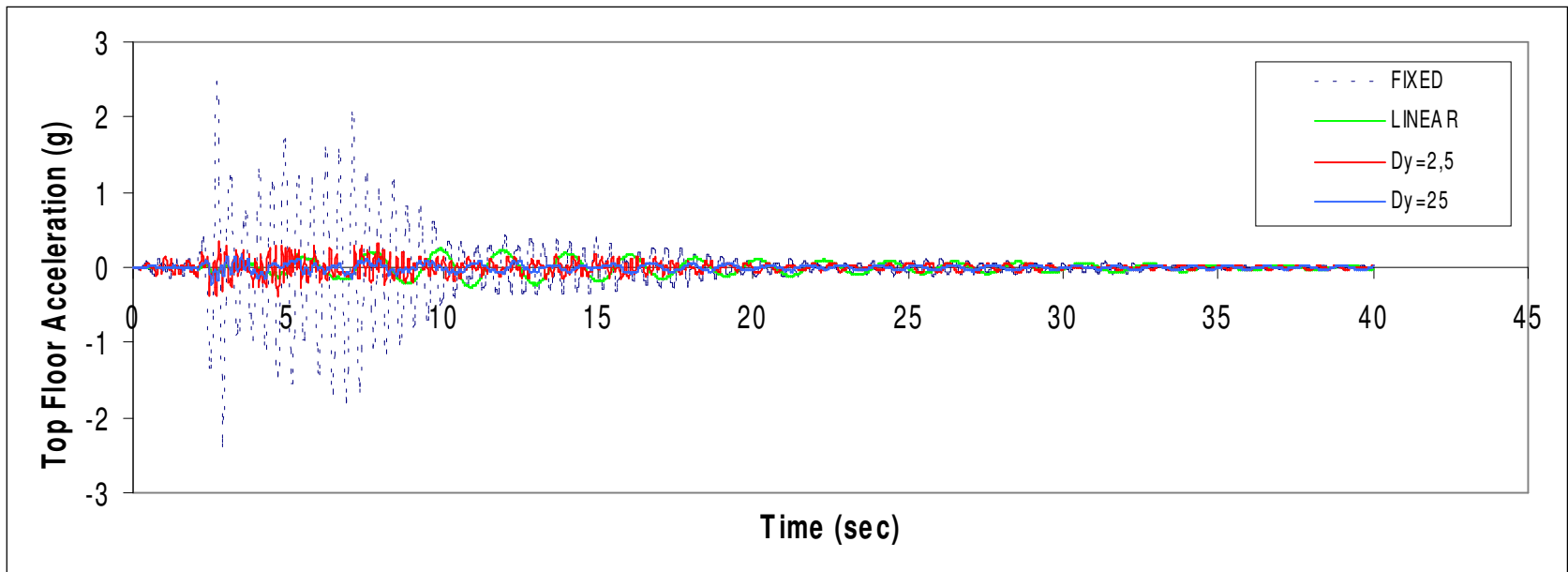


Figure 2.12 Time variation of top floor acceleration under the effect of Loma Prieta (1989) earthquake.

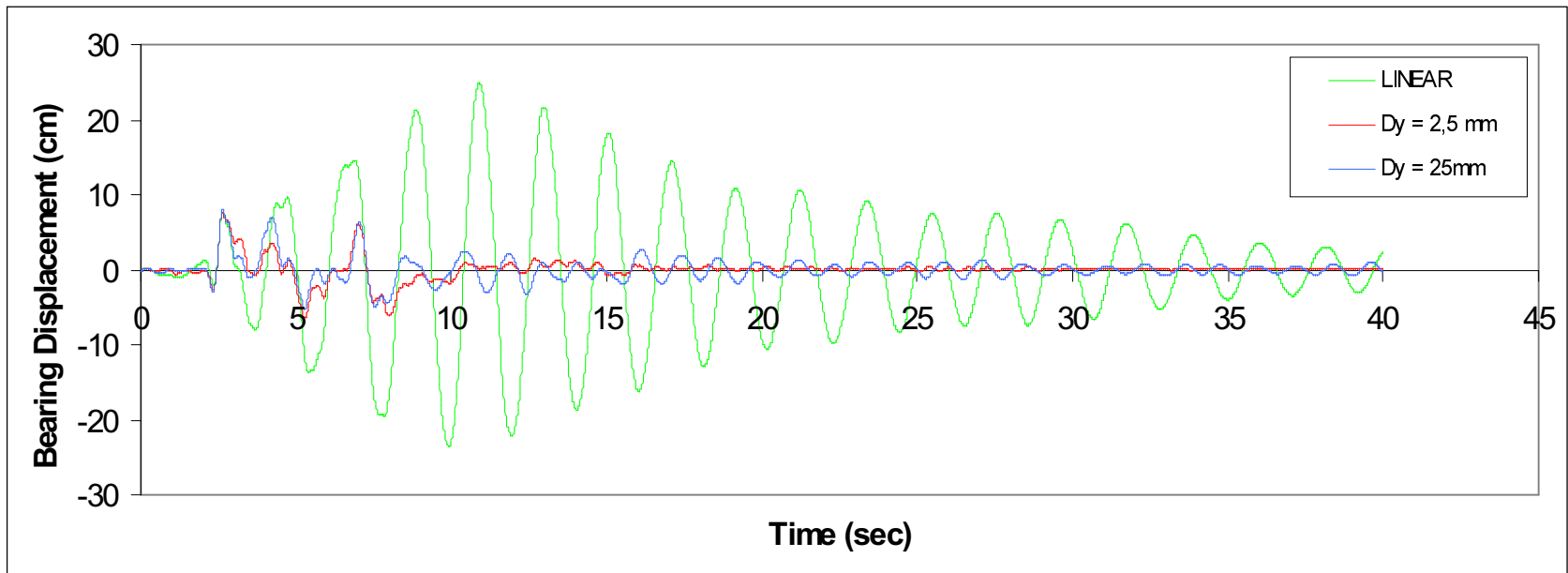


Figure 2.13 Time variation of bearing displacement under the effect of Loma Prieta (1989) earthquake.

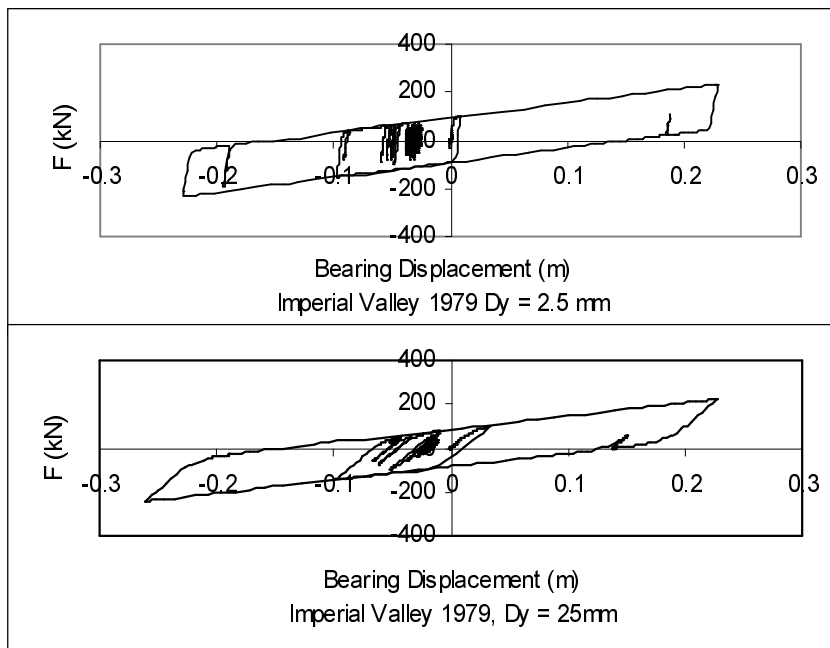


Figure 2.14 Force-deformation behavior for Imperial Valley Earthquake (bilinear hysteretic models)

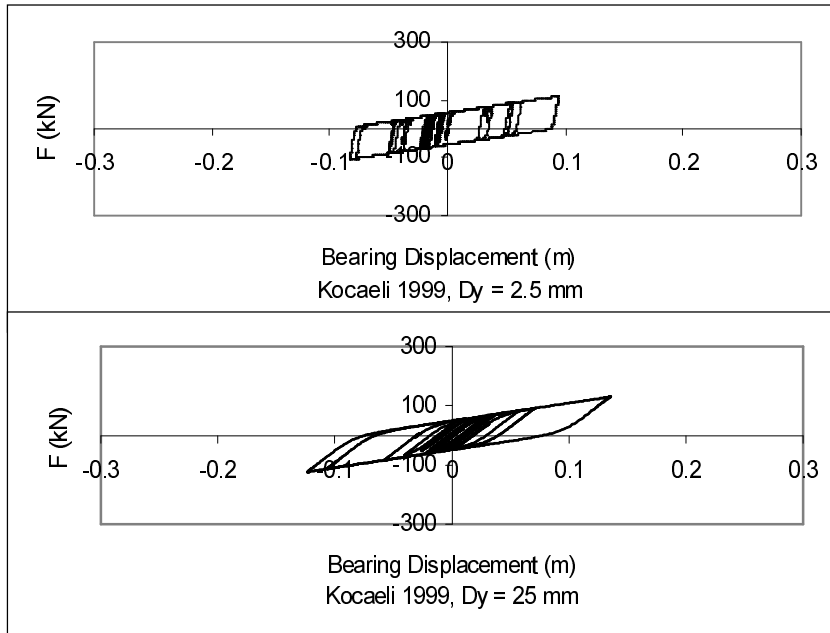


Figure 2.15 Force-deformation behavior for Kocaeli Earthquake (bilinear hysteretic models)

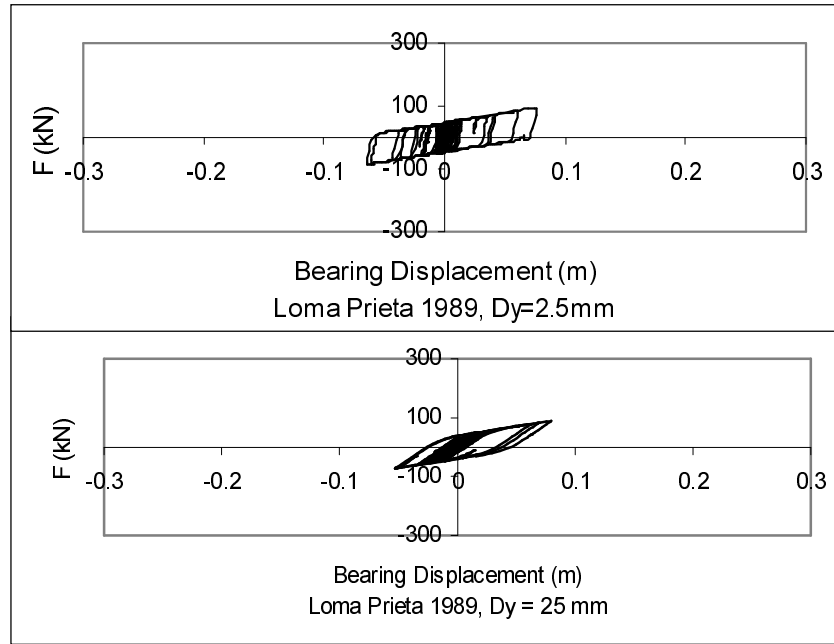


Figure 2.16 Force-deformation behavior for Loma Prieta Earthquake (bilinear hysteretic models)

CHAPTER 3

CASE STUDIES

3.1 Introduction

The aim of the case studies is to investigate the performance features and response mechanisms of base isolated structures for different code specifications. Major characteristics of seismic isolation systems are introduced and studied in the previous chapters. Four different types of buildings are used in the analyses. The isolated buildings are analyzed by using Static Equivalent Lateral Force, Response Spectrum and Time History methods. A commercial computer package, namely SAP2000, is used for 3D analysis of the structures. The analyses of these isolated buildings are done for each soil type that is mentioned in the Turkish Seismic Code (Z1, Z2, Z3, and Z4).

The basic motive in the studies is to identify the similarities and differences between the design code IBC2000, and design specification FEMA 273, and make a comparison between them from the design of base isolated structures point of view.

3.2 Description of the Structures

The structures, used for the analyses, are assumed to be serving as school buildings. The detailed descriptions of the buildings are as follows:

3.2.1 Three-Storey Symmetrical Building (Type-I)

The three-storey building has a regular plan (36m x 12m) as shown in Figure 3.1. The structural system is selected as concrete frames with identical columns of 50/50 centimeters in size, and beams of dimension 40/70 centimeters. Each floor slab has 15 centimeters thickness and the story height is 3 meters. The critical damping ratio of superstructure is taken as 2% for isolated cases.

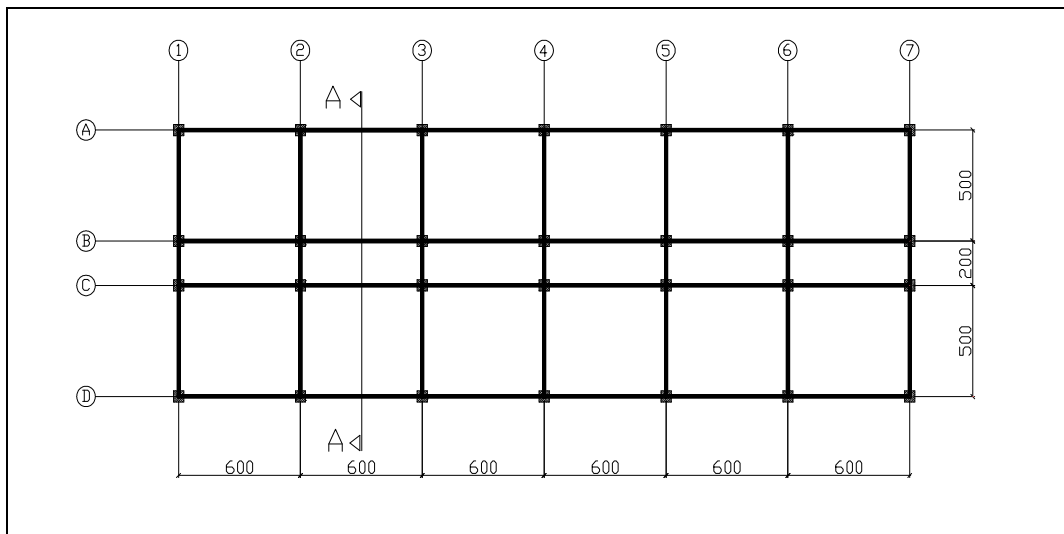


Figure 3.1 Plan view of symmetrical building types.

28 units High Damping Rubber bearings (HDR) are used for the isolation of the building. The detailed calculations of isolation system design are explained in Section 4.1. The bearings have the following linear properties accordingly:

$$\beta_i = 0.15 \quad (\text{isolator damping ratio})$$

$$G = 500 \text{ kN/m}^2$$

$$K_h = 805 \text{ kN/m}$$

$$K_v = 500000 \text{ kN/m}$$

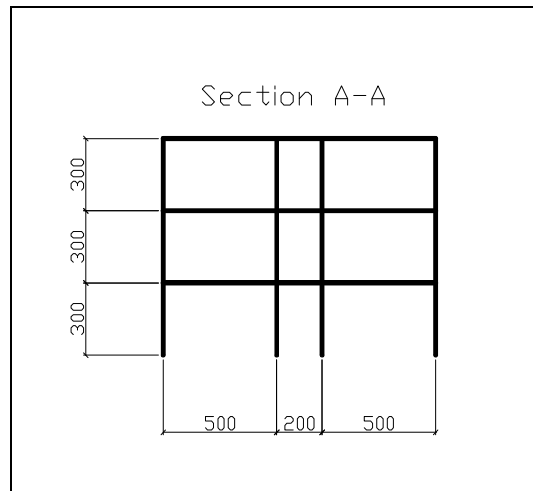


Figure 3.2 Section view of building Type-I

3.2.2 Five-Storey Symmetrical Building (Type-II)

The five-storey building has a regular plan (36m x 12m) as shown in Figure 3.1. The structural system and seismic isolation system is identical with three-storey symmetrical building.

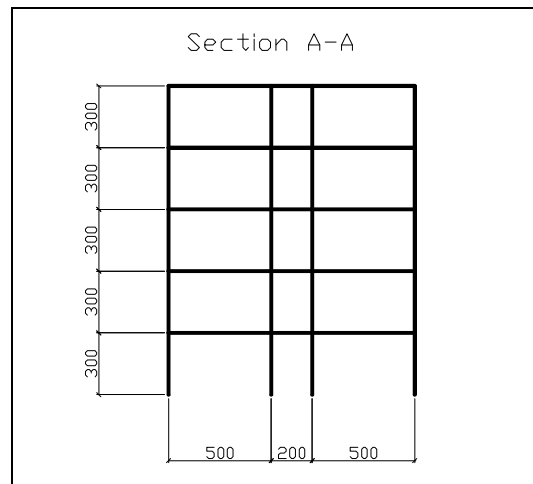


Figure 3.3 Section view of building Type-II

3.2.3 Eight-Storey Symmetrical Building (Type-III)

The eight-storey building has a regular plan (36m x 12m) as shown in Figure 3.1. The structural system and seismic isolation system is identical with three-storey symmetrical building.

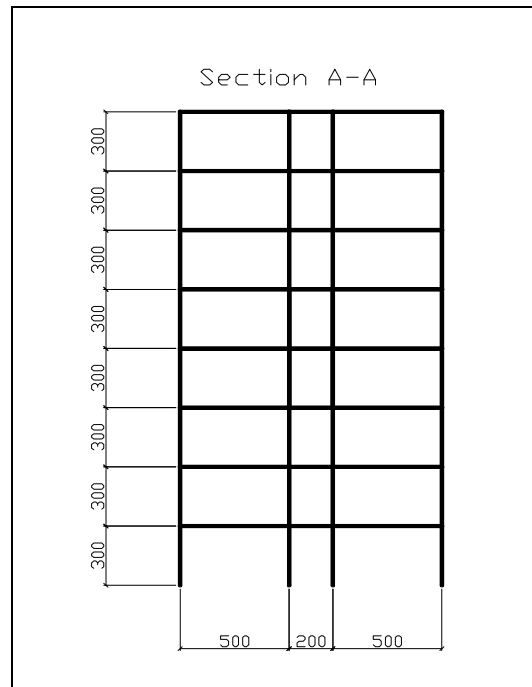


Figure 3.4 Section view of building Type-III

3.2.4 Non-symmetrical Building (Type-IV)

The plan view of five storey non-symmetrical building is shown in Figure 3.5 below. The structural system is selected as concrete frames with identical columns of 50/50 centimeters in size, and beams of dimension 40/70 centimeters. Each floor slab has 15 centimeters thickness and the story height is 3 meters. The critical damping ratio of superstructure is taken as 2% for isolated cases.

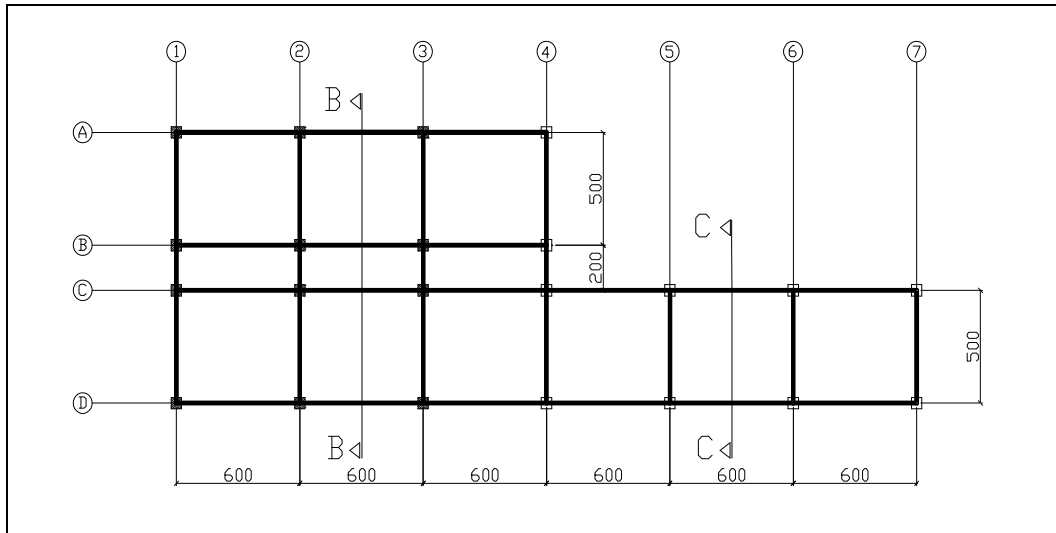


Figure 3.5 Plan view of building Type-IV.

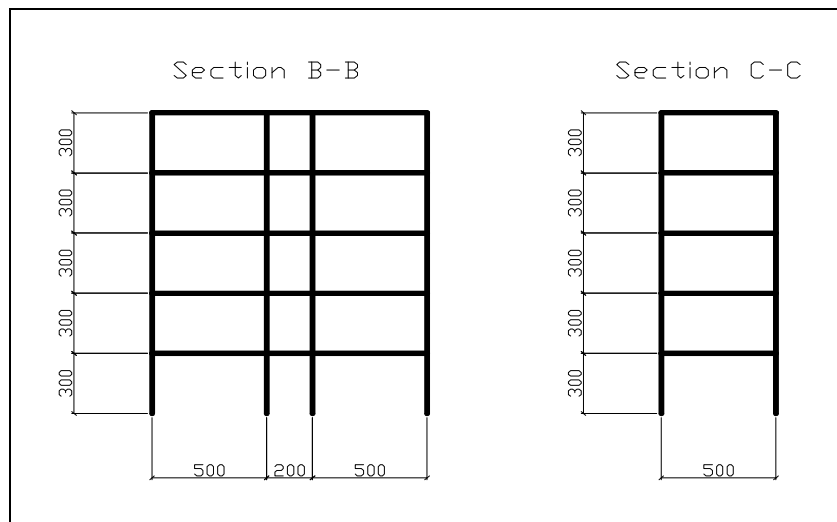


Figure 3.6 Section views of building Type-IV.

22 units High Damping Rubber bearings (HDR) are used for the seismic isolation of the building. The linear properties of the selected isolators are as follows:

$$\beta_i = 0.15 \quad (\text{isolator damping ratio})$$

$$G = 500 \text{ kN/m}^2$$

$$K_h = 805 \text{ kN/m}$$

$$K_v = 500000 \text{ kN/m}$$

3.3 Analysis Methods

In this section, static equivalent lateral force procedure, response spectrum analysis and time history analysis are discussed.

3.3.1 Static Equivalent Lateral Force Procedure

The isolation system should be designed to withstand minimum lateral earthquake displacements, D_D , that act in the direction of each of the main horizontal axes of the structure in accordance with the following [24]:

$$D_D = \left(\frac{g}{4\pi^2}\right) \frac{S_{D1} T_D}{B_D} \quad (3.1)$$

where:

- B_D = Numerical coefficient related to the effective damping of the isolation system at design displacement, as set forth in Table 3.1
- g = Acceleration of gravity
- S_{D1} = Design 5% damped spectral acceleration at 1 sec. period
- T_D = Isolated period at design displacement

Table 3.1 Damping coefficient [11]

EFFECTIVE DAMPING (β_i)	B_D
<2%	0.8
5%	1.0
10%	1.2
20%	1.5
30%	1.7
40%	1.9
>50%	2.0

For damping values other than the one specified in Table 3.1, linear interpolation can be done to find corresponding B_D value. Alternatively, a very close approximation to the table values is given by;

$$\frac{1}{B_D} = 0.25(1 - \ln \beta) \quad (3.2)$$

The effective period of the isolated structure, T_D , is determined as:

$$T_D = 2\pi \sqrt{\frac{W}{K_h g}} \quad (3.3)$$

where W is the total dead load weight of the superstructure.

“The total design displacement, D_{TD} , of elements of the isolation system shall include additional displacement due to actual and accidental torsion calculated considering the spatial distribution of the lateral stiffness of the isolation system and the most disadvantageous location of mass eccentricity. D_{TD} must satisfy the following condition.” [11]:

$$D_{TD} \geq D_D \left[1 + y \left(\frac{12e}{b^2 + d^2} \right) \right] \quad (3.4)$$

where:

- d = Shortest plan dimension
- b = Longest plan dimension
- e = The actual eccentricity measured in plan between the center of mass of the structure and the center of stiffness of the isolation system, plus the accidental eccentricity taken as 5% of the longest plan dimension of the structure perpendicular to the direction of seismic loading under consideration (Figure 3.7).

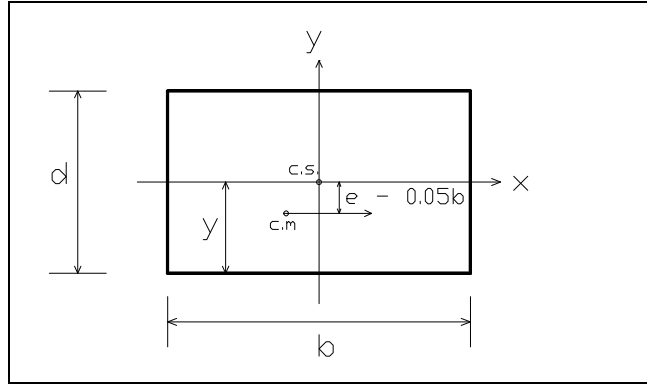


Figure 3.7 Plan dimensions for calculation of D_{TD} [1].

The structure above the isolation system must be designed to withstand a minimum total shear force, V_S :

$$V_S = \frac{K_h D_D}{R} \quad (3.5)$$

where:

R = Seismic load reduction factor.

While FEMA 273 assumes R as equal to one for isolated structures (the structure deforms only in elastic range), IBC2000 takes it as if the structure goes into inelastic range ($1.0 \leq R < 2.0$). In this study R is assumed be equal to one for both of the specifications, thus the lateral EQ force, applied to the building is not reduced. One can easily calculate the corresponding design values of $R=2.0$ if it is desired.

The total shear force, V_S , is distributed over the height of the structure as given by:

$$F_x = \frac{V_S W_x h_x}{\sum_{i=1}^n W_i h_i} \quad (3.6)$$

where:

- h_i = Height above the base to level i.
- h_x = Height above the base to level x.
- W_x = Portion of total dead load that is located at or assigned to level x.
- W_i = Portion of total dead load that is located at or assigned to level i.

3.3.2 Response Spectrum Analysis

The 5% damped spectrum, given in Turkish seismic code (ABYYHY-98, [8]), is used for the analysis of building and the spectrum is modified for each of the soil types (Z1, Z2, Z3, Z4). Spectrum is assumed to be acting on the building from both directions (X-Y) simultaneously. While the component applied from one axis is multiplied by 1.00; the orthogonal component is multiplied by 0.30. According to this logic, two different E.Q. combinations are applied to the structure and the results are examined for each case. In the results, the one, which causes the most critical condition, is taken into account.

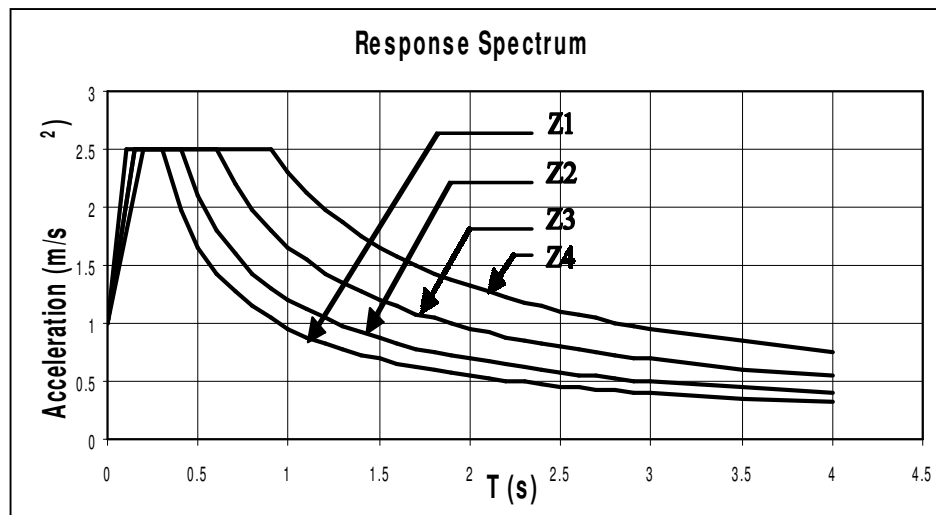


Figure 3.8 Response spectrum functions given in Turkish Seismic Code.

3.3.3 Time History Analysis

“Time history analysis shall be performed with at least three appropriate pairs of horizontal time history components. If three time history analyses are performed, the maximum response of the parameter of interest shall be used for design. If seven or more time history analyses are performed, the average value of the response parameter of interest shall be used for design. Each pair of histories shall be applied simultaneously to the model.” [11]

The used ground motions and their properties are given in Table 3.2 below:

Table 3.2 Ground motions used in time history analyses

	Düzce Earthquake	Marmara Earthquake	Coyote Lake Earthquake	Superstittn Hills Earthquake	Imperial Valley Earthquake	Landers Earthquake	Loma Prieta Earthquake
Place	Düzce, Turkey	Kocaeli, Turkey	Coyote Lake, U.S.A.	Superstittn Hills, U.S.A.	Imperial County, U.S.A.	Yucca Valley, U.S.A.	Santa Cruz County, U.S.A.
Date	12.11.1999	17.08.1999	06.08.1979	24.11.1987	15.10.1979	28.06.1992	17.10.1989
Magnitude (M_w)	7.2	7.4	5.7	6.7	6.6	7.4	7.1
Closest Distance to Fault Rupture (km)	8.23	3.28	3.20	4.30	27.03	9.00	18.00
Number of Data Points	5180	7001	5764	2221	1845	4000	2000
Time Interval (sec.)	0.005	0.005	0.005	0.01	0.02	0.02	0.02

3.4 Design Codes

Since there are no provisions available in the Turkish seismic code for design of base isolated structures; in this study the design procedure for isolated buildings is primarily based on International Building Code 2000 (IBC2000) [11] and Federal Emergency Management Agency (FEMA 273) [17] provisions.

The applicable methods in IBC2000 and FEMA 273 for the design of an isolated building and necessary formulas of these methods are mentioned above. In addition, some important limiting regulations in the design procedure are also stated in the IBC2000 and FEMA 273.

In both IBC2000 and FEMA 273, it is stated that the conditions of site where the structure is located must be reflected into the design procedure. Consequently, the calculated response of the structure is modified. A coefficient called as scaling factor is involved in design calculations for this purpose. In the following paragraphs, scaling concept was given for both of the codes.

3.4.1 IBC2000

The base shear, V_S , is taken as not less than the following threshold values for static equivalent lateral force procedure:

- The lateral seismic force required for a fixed-base structure of the same weight and a period equal to the isolated period.
- The base shear corresponding to the factored design wind load.
- The lateral seismic load required to exceed the isolation system (the yield level of a softening system, the break away friction level of a sliding system factored by 1.5).

When the factored base shear force on structural elements, determined using either response spectrum or time history analysis, is less than the minimum prescribed below, response parameters, including member forces and moments, is adjusted proportionally upward.

- The total design displacement of isolation system is taken as not less than 90% of D_{TD} as specified in Equation 3.4.

- The design base shear force on the structure above the isolation system, if regular in configuration, is taken as not less than 80% of V_S as prescribed by Equation 3.5.

In IBC2000 there are two exceptions for the above conditions:

1. The design base shear force on the structure above the isolation system, if regular in configuration, is permitted to be taken as less than 80%, but not less than 60% of V_S , provided time history analysis is used for design of the structure. The design base shear force on the structure above the isolation system, if irregular in configuration, must be taken as not less than V_S .
2. The design base shear force on the structure above the isolation system, if irregular in configuration, is permitted to be taken as less than 100%, but not less than 80% of V_S , provided time history analysis is used for design of the structure.

The scaling limits on displacements specified above must be evaluated using values of D_{TD} determined in accordance with Equation 3.4 except that $D_{D'}$ is permitted to be used instead of D_D where $D_{D'}$ is prescribed by the following formula:

$$D_{D'} = \frac{D_D}{\sqrt{1 + \left(\frac{T}{T_D}\right)^2}} \quad (3.7)$$

where:

- T = Elastic, fixed-based period of the structure above the isolation system.
- T_D = Effective period, in seconds, of the seismically isolated structure at the design displacement in the direction under consideration as prescribed by Equation 3.3.

Table 3.3 Scaling limits for IBC2000

		If Response Spectrum is Used	If Time History Analysis is Used
Regular	V_s	$\geq 0.8 V_s$	$\geq 0.6 V_s$
	D_{TD}	$\geq 0.9 D_{TD}$	$\geq 0.9 D_{TD}$
Irregular	V_s	$\geq 1.0 V_s$	$\geq 0.8 V_s$
	D_{TD}	$\geq 0.9 D_{TD}$	$\geq 0.9 D_{TD}$

3.4.2 FEMA 273

The value of V_s is taken as not less than the following for static equivalent lateral force procedure:

- The base shear corresponding to the factored design wind load.
- The lateral seismic load required to fully activate the isolation system factored by 1.5 (include the yield level of a softening system, the break away friction level of a sliding system).

If the total design displacement determined by response spectrum analysis is found to be less than the value of D_{TD} prescribed by Equation 3.4, then all response parameters, including component actions and deformations, must be adjusted upward proportionally to the D_{TD} value and used for design.

If the design displacement determined by time history analysis is less than the value of D_D prescribed by Equation 3.7, then all response parameters, including component actions and deformations, must be adjusted upward proportionally to the D_D value and used for design.

CHAPTER 4

ISOLATION SYSTEM DESIGN

4.1 Design of High Damping Rubber Bearing

As an example of isolation system design, the symmetrical building, introduced in Section 3.2.2, is considered. The designed HDR bearings are used also for the other building types analyzed in the case studies.

Twenty-eight HDR bearings are used for the isolation of the building. The selected strategy for the design is to use one type of bearing for the whole system. The basic structural data to be used for the design is as follows:

$T_D = 2.00$ sec.	(Target period for 'Design Level' earthquake)
$T_M = 2.50$ sec.	(Target period for 'Max. Capable Level' earthquake)
$R = 1.00$	(Seismic load reduction factor)
$G = 500$ kN/m ²	(For large shear strains)
$G = 700$ kN/m ²	(For small shear strains)
$K = 2,000,000$ kN/m ²	(Bulk modulus)
$\beta_i = 15\%$	(Damping ratio of isolator)
$W_T = 22330$ kN	(Total weight of the structure)
$\gamma_{max} = 150\%$	

The site is assumed to be located in seismic zone 1 with Z1 soil type.

In [1], it is stated that: “Seismic faults are grouped into three categories based on the seriousness of the hazard they represent. Faults capable of producing large magnitude earthquakes ($M > 7.0$) and have a high rate of seismic activity (annual average seismic slip rate, SR, of 5 mm or more) are classified as type A sources. Faults capable of producing moderate magnitude earthquakes ($M < 6.5$) with a relatively low rate of seismic activity ($SR < 2$ mm) are classified as type C sources. All faults other than types A and C are classified as type B sources”.

The distance of the site to the nearest active fault is assumed to be less than 2 km; and the fault type is assumed to be type A. As a result of these conditions S_{D1} is equal to 0.64.

4.1.1 Lateral Stiffness of Base Isolators

By using Equation 3.3 for ‘Design Level Earthquake’:

$$2.00 = 2\pi \sqrt{\frac{22330}{k_{total} \cdot 9.81}} \quad \rightarrow \quad k_{total} = 22465.7 \text{ kN/m}$$

$$k_D = \frac{22465.7}{28} = 802.35 \text{ kN/m} \quad (\text{for one bearing})$$

For ‘Maximum Capable Earthquake Level’:

$$2.50 = 2\pi \sqrt{\frac{22330}{k_{total} \cdot 9.81}} \quad \rightarrow \quad k_{total} = 14378 \text{ kN/m}$$

$$k_M = \frac{14378}{28} = 513.50 \text{ kN/m} \quad (\text{for one bearing})$$

where k_D and k_M are the minimum lateral stiffness of base isolation bearings corresponding to the ‘design earthquake’ and ‘maximum capable earthquake’, respectively.

4.1.2 Estimation of Lateral Displacements

From Equation 3.1

$$D_D = \left(\frac{9.81}{4\pi^2}\right) \frac{0.64 \times 2.00}{1.38} = 0.23 \text{ m}$$

$$D_M = \left(\frac{9.81}{4\pi^2}\right) \frac{0.64 \times 2.50}{1.38} = 0.29 \text{ m}$$

where D_D and D_M are the displacements of the isolation system corresponding to the ‘design earthquake’ and ‘max. capable earthquake’, respectively. The damping reduction factor $B=1.38$ is obtained from Equation 3.2.

4.1.3 Estimation of Disc Dimensions

Thickness of the disc can be calculated by,

$$t_r = \frac{D_D}{\gamma_{\max}} \tag{4.1}$$

Therefore

$$t_r = \frac{0.23}{1.5} = 0.153 \text{ m}$$

Take

$$t_r = 20 \text{ cm}$$

Disc diameter, Φ , is estimated by using Equation 2.1,

$$A = \frac{802.35 \times 0.2}{500} = 0.321 \text{ m}^2$$

$$\Phi = 0.639 \text{ m}$$

Take

$$\Phi = 64 \text{ cm} \quad A = 0.322 \text{ m}^2$$

4.1.4 Actual Bearing Stiffness & Revised Fundamental Period

$$k_D = \frac{0.322 \times 500}{0.2} = 805 \text{ kN/m}$$

$$k_{total} = 28 \times 805 = 22540 \text{ kN/m}$$

$$T_D = 2\pi \sqrt{\frac{22330}{22540 \times 9.81}} = 1.997 \text{ sec.}$$

It is seen that the calculated revised value of $T_D = 1.997$ sec. is very close to the target period of $T = 2.00$ sec.

4.1.5 Bearing Detail

For compressive stresses under vertical loads, the isolators undergo relatively smaller shear strains on the order of $\gamma = 0.20$. Therefore $G = 700 \text{ kN/m}^2$ should be used. Shape factor, S , is selected as 8. The compression modulus, E_c , from Equation 2.4 is:

$$E_c = \frac{6 \times 700 \times 8^2 \times 2000000}{6 \times 700 \times 8^2 + 2000000} = 236,953.45 \text{ kN/m}^2$$

where the total vertical stiffness is determined from Equation 2.2 as,

$$k_v = \frac{0.322 \times 28 \times 236953.45}{0.20} = 10,681,861.5 \text{ kN/m}$$

The vertical displacement, Δt_v , becomes;

$$\Delta t_v = \frac{W}{k_v} = \frac{22330}{10681861.5} = 2.09 \times 10^{-3} \text{ m}$$

The vertical fundamental period of vibration is given by;

$$T_v = \frac{T_H}{\sqrt{6S}} \tag{4.2}$$

gives,

$$T_v = \frac{2.00}{\sqrt{6 \times 8}} = 0.102 \text{ sec.}$$

As a result $S = 8$ is adequate.

$$S = \frac{\Phi}{4t_o} \tag{4.3}$$

where t_o is the thickness of single layer of rubber.

$$t_o = \frac{640}{4 \times 8} = 20 \text{ mm}$$

$$n \times t_o = 200 \text{ mm}$$

$$n = 10 \text{ layers}$$

Consequently, the design of the bearing is completed as shown in Figure 4.1. The end plates are 25mm thick, and the steel shims are 2mm each. The total height is:

$$h = (2 \times 25) + (10 \times 20) + (9 \times 2) = 268 \text{ mm}$$

The steel shims will have a diameter $\Phi_s = 630 \text{ mm}$, giving 5mm cover.

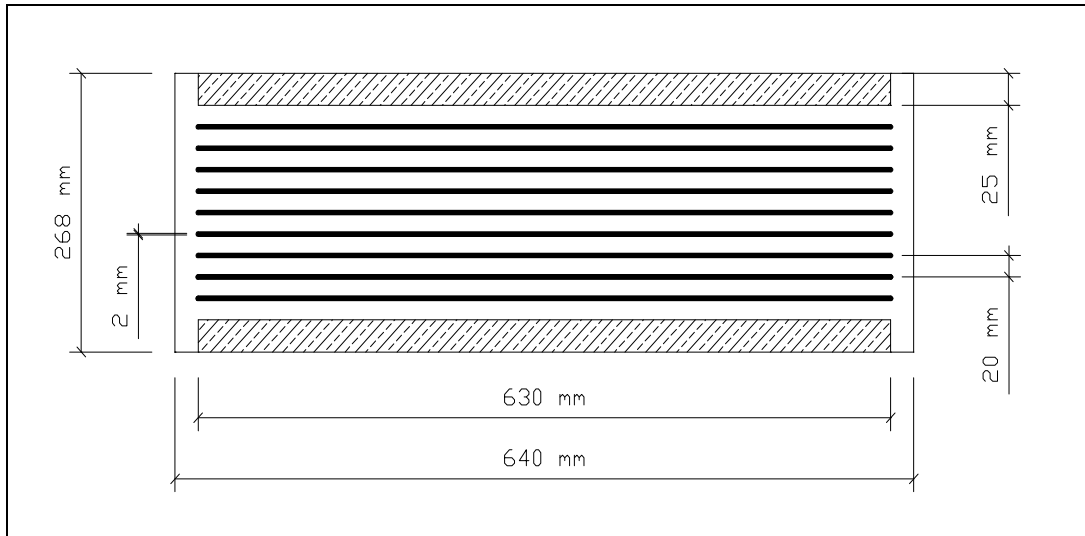


Figure 4.1 Detail design of isolator.

4.1.6 Buckling Load

$$P_{cr} = \sqrt{P_S P_E} \quad (4.4)$$

$$P_S = GA \quad (4.5)$$

$$P_E = \frac{\pi^2 (EI)_{eff}}{t_r^2} \quad (4.6)$$

$$(EI)_{eff} = \frac{1}{3} E_C I \quad (4.7)$$

$$\rightarrow P_{cr} = \sqrt{\frac{0.322 \times 500 \times \pi^2 \times 236953.45 \times \pi \times 0.32^4 \times 0.25}{3 \times 0.2^2}} = 5083 \text{ kN}$$

Maximum vertical load for one isolator is calculated from tributary area:

$$(F_V)_{\max} = \frac{6 \times 3.5}{36 \times 12} \times 22330 = 1085.5 \text{ kN}$$

$$\text{Factor of Safety, } FS = \frac{5083}{1085.5} = 4.68$$

4.2 Performance Comparison of Isolation Systems

The design of a seismic isolation system involves many interrelated variables such as targeted period of the isolated structure, base shear and damping of isolation system. To illustrate an overview of how these variables affect the structural design, the IBC2000 requirements for isolated buildings is used.

In the code, the displacement across the isolators (D_D), the isolation period (T_D) and the base shear (V_S) are given by Equations 3.1, 3.3, and 3.5. It is clear from Equations 3.1 and 3.5 that the damping provided by the isolation system reduces both the base shear and isolator displacement.

In order to compare the impact of the variables, involved in design procedure, on the performance of isolation systems with different damping values; a basis must be established. There are three alternatives cases;

- The seismic isolation systems have the same base shear.
- The seismic isolation systems have the same displacement.
- The seismic isolation systems have the same isolated period.

Each of these alternatives is evaluated with regard to their overall impact. In order to be able to easily follow, numerical comparison of a 10% damped ($B_D = 1.2$), a 15% damped ($B_D = 1.35$), and a 20% damped ($B_D = 1.5$) systems is discussed. 10%, 15%, and 20% damping values are selected for the comparison since they are in the practical range of currently available systems.

Equal Base Shear

When the base shear of two isolated systems is equal, the relationships for isolation period and displacement can be derived from Equations 3.1, 3.3 and 3.5.

$$V_1 = V_2$$

$$T_1 = \frac{T_2}{r}$$

$$D_1 = \frac{D_2}{r^2}$$

where $r = \frac{B_1}{B_2}$

B_1 and B_2 are the damping factors for the two isolation systems. To state these relations numerically:

$$V_{10} = V_{20}$$

$$T_{10} = 1.25 T_{20}$$

$$D_{10} = 1.56 D_{20}$$

$$V_{15} = V_{20}$$

$$T_{15} = 1.11 T_{20}$$

$$D_{15} = 1.24 D_{20}$$

From Figure 4.2 it is seen that for an equal base shear, 10% and 15% damped systems will require 25% and 11% longer periods and will produce 1.56 and 1.24 times the displacements of a 20% damped system.

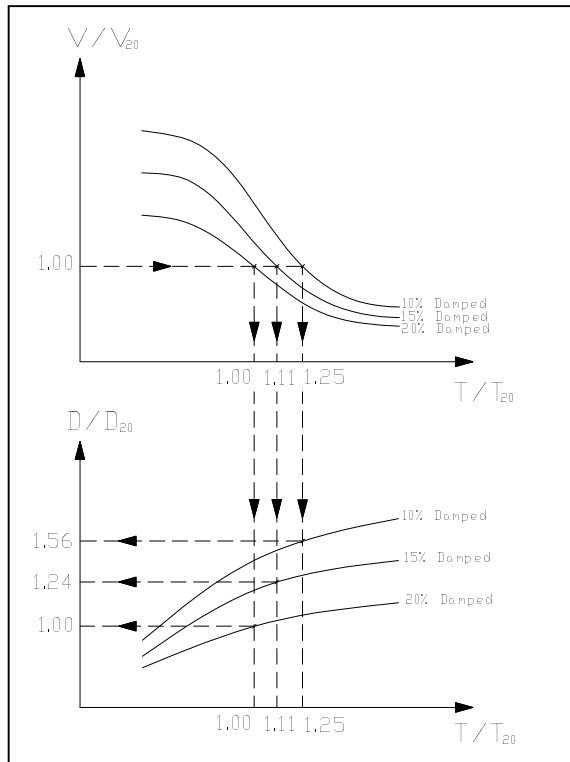


Figure 4.2 Effect of damping for equal base shear case.

Equal Isolated Periods

When the isolated period of two systems is equal, the relationships for base shear and displacement can be derived from Equations 3.1, 3.3 and 3.5.

$$T_1 = T_2$$

$$V_1 = \frac{V_2}{r}$$

$$D_1 = \frac{D_2}{r}$$

To state these relations numerically:

$$T_{10} = T_{20}$$

$$V_{10} = 1.25 V_{20}$$

$$D_{10} = 1.25 D_{20}$$

$$T_{15} = T_{20}$$

$$V_{15} = 1.11 V_{20}$$

$$D_{15} = 1.11 D_{20}$$

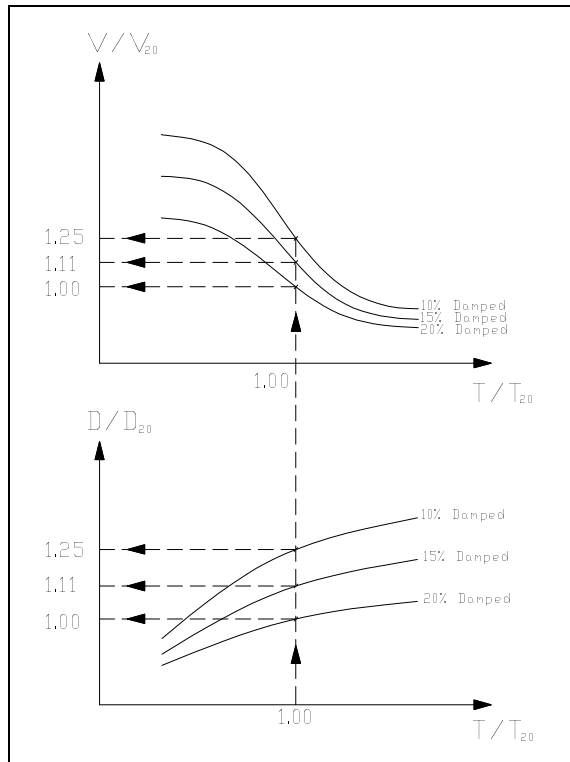


Figure 4.3 Effect of damping for equal period case.

For an equal isolated period, while 10% damped system will produce 25% greater displacement and base shear, 15% damped system will produce 11% greater displacement and base shear when compared to 20% damped system.

Equal Displacements

When the displacements of two isolated systems are equal, the relationships for isolation period and base shear can be derived from Equations 3.1, 3.3 and 3.5.

$$D_1 = D_2$$

$$T_1 = r.T_2$$

$$V_1 = \frac{V_2}{r^2}$$

To state these relations numerically:

$$D_{10} = D_{20}$$

$$T_{10} = 0.8 T_{20}$$

$$V_{10} = 1.56 V_{20}$$

$$D_{15} = D_{20}$$

$$T_{15} = 0.9 T_{20}$$

$$V_{15} = 1.24 V_{20}$$

Thus, for an equal displacement, 10% and 15% damped systems will require 20% and 10% lower periods and will produce 1.56 and 1.24 times the base shear of a 20% damped system.

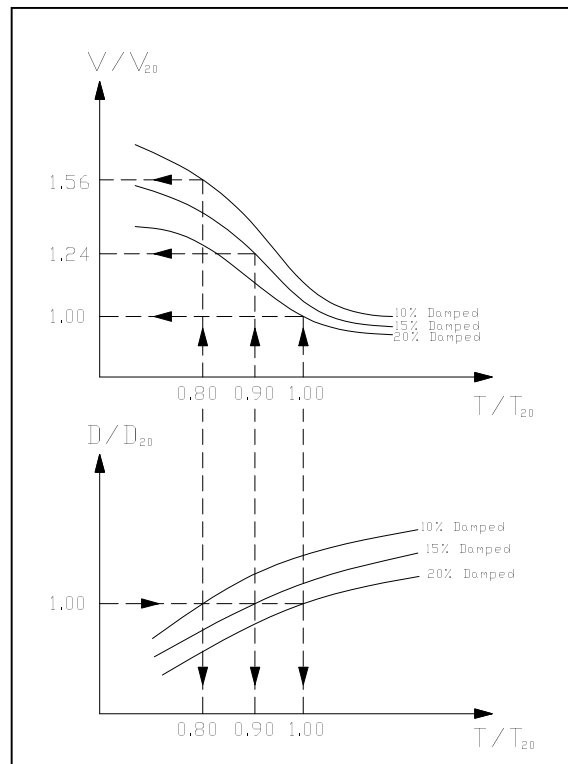


Figure 4.4 Effect of damping for equal displacement case.

CHAPTER 5

ANALYSIS & DISCUSSION OF RESULTS

5.1 Analysis of the Base Isolated Symmetrical Building

In this section “scaling” phenomenon mentioned in FEMA-273 & IBC2000 and the differences between these two codes from the “scaling” point of view are discussed for the symmetric buildings. To facilitate a study of the code provisions, building Types I, II and III are selected. The description of the buildings is introduced in Section 3.2. The high damping rubber bearings, HDR, designed in Section 4.1 are used for the isolation of the all buildings. Response spectrum analysis, described in Section 3.3.2, is carried out on building Types I, II and III. In addition, static equivalent lateral force and time history analyses, described in Section 3.3.1 and 3.3.3, are performed for Type II which typifies the class of symmetrical structure that is encountered in design. The analyses of the isolated buildings are done for each soil type that is given in the Turkish Seismic Code (Z1, Z2, Z3, and Z4).

5.1.1 Scaling of the Results

The results of the analyses are scaled according to both FEMA-273 and IBC2000 as mentioned in Section 3.4. The detailed calculation of scaling factors for each analysis method is given below.

5.1.1.1 Scaling for Static Equivalent Lateral Force Procedure

The limits of scaling mentioned in FEMA-273 and IBC2000 for static equivalent lateral force procedure are the same except that an additional limit is defined in IBC2000: “The base shear must be greater than the lateral seismic force required for a fixed-base structure of the same weight and a period equal to the isolated period”.

Building Type-II is analyzed with static equivalent lateral force procedure and the results of the analysis are scaled according to the mentioned limit. For the calculation of the lateral seismic force, V_T , the procedure described in Turkish Seismic Code is used.

$$V_T = \frac{W_T \times A(T_1)}{R(T_1)} > 0.10 \times I \times W_T \quad (5.1)$$

$$A(T_1) = A_0 \times I \times S(T_1) \quad (5.2)$$

$$A_0 = 0.40$$

$$I = 1.4$$

$$R = 8 \text{ (Seismic load reduction factor for non-isolated building)}$$

$$W_T = 22330 \text{ kN}$$

$$T_D = 2.09 \text{ sec.}$$

Table 5.1 Calculation of scaling factor for Type-II according to IBC2000

	S(T)	A(T) (Equation 5.2)	V_T (kN) (Equation 5.1)	V_S (kN) (Equation 3.5)	Scaling Factor
Z1	0.529	0.296	826	5432	no need to scale
Z2	0.666	0.373	1041	6790	no need to scale
Z3	0.921	0.516	1440	9670	no need to scale
Z4	1.274	0.713	1990	11027	no need to scale

5.1.1.2 Scaling for Response Spectrum Analysis

Building Types I, II and III are analyzed with response spectrum analysis and the results of the analysis are scaled according to both FEMA-273 and IBC2000. To be comprehensible, the parameters needed for the calculation of scaling factors are given below. The damping coefficient, B_D , is taken as 1.38 for the calculations since the HDR, bearings designed in Section 4.1, are used for the isolation. As a result of the modal analysis the fixed based period T , and isolated period T_D of the buildings are determined as:

Table 5.2 Fixed and isolated periods of buildings

	Type-I	Type-II	Type-III
T (sec.)	0.27	0.45	1.57
T_D (sec.)	1.57	2.09	2.73

Scaling according to IBC2000:

When IBC2000 is considered, the design displacement determined by response spectrum analysis, $D_{analysis}$, must be greater than 90% of D_{TD} , as specified in Equation 3.4. On the other hand, the design base shear force on the structure above the isolation system must be greater than 80% of V_S as prescribed by Equation 3.5. Otherwise, all response parameters, including inertial forces and deformations, must be adjusted proportionally upward.

When the results of the analyses are examined, it is seen that the first scaling limit, $D_{analysis} > 0.9 \times D_{TD}$, is more critical than the second one and results in greater scaling factors. Therefore, displacement dependent scaling limit is used in the scaling factor calculations.

Table 5.3 Calculation of scaling factor for Type-I according to IBC2000

	S_{D1}	D_D (cm) (Equation 3.1)	$D_{D'}$ (cm) (Equation 3.7)	$0,9*D_{TD'}$ (cm) (Equation 3.4)	$D_{analysis}$ (cm)	Scaling Factor
Z1	0.64	18.09	17.84	20.39	15.14	1.347
Z2	0.80	22.62	22.30	25.49	19.06	1.337
Z3	1.14	32.23	31.78	36.33	26.36	1.378
Z4	1.30	36.75	36.24	41.42	36.46	1.136

Table 5.4 Calculation of scaling factor for Type-II according to IBC2000

	S_{D1}	D_D (cm) (Equation 3.1)	$D_{D'}$ (cm) (Equation 3.7)	$0,9*D_{TD'}$ (cm) (Equation 3.4)	$D_{analysis}$ (cm)	Scaling Factor
Z1	0.64	24.10	23.56	26.93	21.01	1.282
Z2	0.80	30.13	29.45	33.66	26.44	1.273
Z3	1.14	42.90	41.94	47.94	36.60	1.310
Z4	1.30	48.92	47.82	54.66	50.60	1.080

Table 5.5 Calculation of scaling factor for Type-III according to IBC2000

	S_{D1}	D_D (cm) (Equation 3.1)	$D_{D'}$ (cm) (Equation 3.7)	$0,9*D_{TD'}$ (cm) (Equation 3.4)	$D_{analysis}$ (cm)	Scaling Factor
Z1	0.64	31.46	27.24	31.14	28.00	1.112
Z2	0.80	39.33	34.05	38.92	35.43	1.099
Z3	1.14	56.04	48.52	55.46	48.80	1.136
Z4	1.30	63.91	55.33	63.24	67.40	no need to scale

Scaling according to FEMA-273:

When the FEMA-273 is considered, the design displacement determined by response spectrum analysis, $D_{analysis}$, must be greater than the value of D_{TD} prescribed by Equation 3.4. Otherwise, all response parameters, including component actions and deformations, must be adjusted upward proportionally to the D_{TD} value and used for design.

Table 5.6 Calculation of scaling factor for Type-I according to FEMA-273

	S_{D1}	D_D (cm) (Equation 3.1)	D_{TD} (cm) (Equation 3.4)	$D_{analysis}$ (cm)	Scaling Factor
Z1	0.64	18.09	22.97	15.14	1.517
Z2	0.80	22.62	28.73	19.06	1.507
Z3	1.14	32.23	40.93	26.36	1.553
Z4	1.30	36.75	46.67	36.46	1.280

Table 5.7 Calculation of scaling factor for Type-II according to FEMA-273

	S_{D1}	D_D (cm) (Equation 3.1)	D_{TD} (cm) (Equation 3.4)	$D_{analysis}$ (cm)	Scaling Factor
Z1	0.64	24.10	30.61	21.01	1.457
Z2	0.80	30.13	38.26	26.44	1.447
Z3	1.14	42.90	54.49	36.60	1.489
Z4	1.30	48.92	62.13	50.60	1.228

Table 5.8 Calculation of scaling factor for Type-III according to FEMA-273

	S_{D1}	D_D (cm) (Equation 3.1)	D_{TD} (cm) (Equation 3.4)	$D_{analysis}$ (cm)	Scaling Factor
Z1	0.64	31.46	39.95	28.00	1.427
Z2	0.80	39.33	49.95	35.43	1.410
Z3	1.14	56.04	71.17	48.80	1.458
Z4	1.30	63.91	81.17	67.40	1.204

5.1.1.3 Scaling for Time History Analysis

Building Type II is analyzed with time history analysis and the results of the analysis are scaled according to both FEMA-273 and IBC2000. The parameters needed for the calculation of scaling factors are given below. The damping coefficient, B_D , is taken

as 1.38 for the calculations since the HDR, bearings designed in Section 4.1, are used for the analysis. The fixed based, T , and isolated periods, T_D , of the building are given in Table 5.2.

Scaling according to IBC2000

The displacement dependent scaling limit for time history analysis is same with the one given for response spectrum analysis. However, the design base shear force on the structure above the isolation system must be greater than 60% of V_S as prescribed by Equation 3.5. Otherwise, all response parameters, including component actions and deformations, must be adjusted proportionally upward.

When the results of the analyses are examined, it is seen that the first scaling limit, $D_{analysis} > 90\%$ of $D_{TD'}$, is more critical than the second one and results in greater scaling factors. Therefore, it is used in the scaling factor calculations.

Table 5.9 Calculation of scaling factor for Type-II according to IBC2000

	S_{D1}	D_D (cm) (Equation 3.1)	$D_{D'}$ (cm) (Equation 3.7)	$0,9*D_{TD'}$ (cm) (Equation 3.4)	$D_{analysis}$ (cm)	Scaling Factor
Z1	0.64	24.10	23.56	26.93	30.80	no need to scale
Z2	0.80	30.13	29.45	33.66	30.80	1.093
Z3	1.14	42.90	41.94	47.94	30.80	1.557
Z4	1.30	48.92	47.82	54.66	30.80	1.775

Scaling according to FEMA-273

When the FEMA-273 is considered, the design displacement determined by time history analysis, $D_{analysis}$, must be greater than the value of $D_{D'}$ prescribed by Equation 3.7. Otherwise, all response parameters, including component actions and deformations, must be adjusted upward proportionally to the $D_{D'}$ value and used for design.

Table 5.10 Calculation of scaling factor for Type-II according to FEMA-273

	S_{D1}	D_D (cm) (Equation 3.1)	$D_{D'}$ (cm) (Equation 3.7)	$D_{analysis}$ (cm)	Scaling Factor
Z1	0.64	24.10	23.56	30.80	no need to scale
Z2	0.80	30.13	29.45	30.80	no need to scale
Z3	1.14	42.90	41.94	30.80	1.362
Z4	1.30	48.92	47.82	30.80	1.553

5.1.2 Results of the Analyses

The results of the analyses of building Type-II, representing the typical symmetrical structure, are given in Table 5.11 below; also in order to be able to compare different analysis methods a comparison table, Table 5.12, is prepared. It can be concluded from the comparison table that response spectrum analysis, scaled according to FEMA-273 provisions, results in the most conservative design values.

Table 5.11 Results of the analyses for Type-I

		<i>T</i> (sec)	<i>Base Shear in X Direction</i> VX (kN)	<i>Base Shear in Y Direction</i> VY (kN)	<i>Base Moment in X Direction</i> MX (kN.m)	<i>Base Moment in Y Direction</i> MY (kN.m)	<i>Max. Interstory Drift Ratio</i>	<i>Max. Isolator Displacement</i> (cm)		
FEMA-273	TIME HISTORY	Z1	1.57	4614	5160	29113	26169	0.0050	23.1	NO NEED TO SCALE
		Z2	1.57	4614	5160	29113	26169	0.0050	23.1	
		Z3	1.57	6294	7039	39651	35641	0.0070	31.4	RESULTS ARE SCALED
		Z4	1.57	7174	7963	45295	40715	0.0078	35.9	
	RESPONSE SPECTRUM	Z1	1.57	5148	5147	29112	29108	0.0053	23.0	RESULTS ARE SCALED
		Z2	1.57	6438	6438	36408	36404	0.0066	28.7	
		Z3	1.57	9178	9177	51897	51891	0.0095	40.9	
		Z4	1.57	10461	10461	59155	59149	0.0108	46.7	
	EQUIVALENT LATERAL	Z1	1.57	4076	4076	27970	27970	0.0045	21.8	NO NEED TO SCALE
		Z2	1.57	5093	5093	34962	34962	0.0051	25.0	
		Z3	1.57	7253	7253	49788	49788	0.0074	37.9	
		Z4	1.57	8270	8270	56774	56774	0.0089	44.3	
IBC2000	TIME HISTORY	Z1	1.57	4614	5160	29113	26169	0.0050	23.1	NO NEED TO SCALE
		Z2	1.57	5091	5696	31819	28602	0.0057	25.5	
		Z3	1.57	7246	8115	45328	41077	0.0081	36.3	RESULTS ARE SCALED
		Z4	1.57	8275	9251	51674	46830	0.0092	41.4	
	RESPONSE SPECTRUM	Z1	1.57	4571	4571	25849	25846	0.0047	20.4	RESULTS ARE SCALED
		Z2	1.57	5712	5712	32301	32297	0.0059	25.5	
		Z3	1.57	8143	8143	46049	46043	0.0084	36.3	
		Z4	1.57	9285	9284	52500	52494	0.0096	41.4	
	EQUIVALENT LATERAL	Z1	1.57	4076	4076	27970	27970	0.0045	21.8	NO NEED TO SCALE
		Z2	1.57	5093	5093	34962	34962	0.0051	25.0	
		Z3	1.57	7253	7253	49788	49788	0.0074	37.9	
		Z4	1.57	8270	8270	56774	56774	0.0089	44.3	

Table 5.12 Results of the analyses for Type-II

		<i>T</i> (sec)	<i>Base Shear in X Direction</i> VX (kN)	<i>Base Shear in Y Direction</i> VY (kN)	<i>Base Moment in X Direction</i> MX (kN.m)	<i>Base Moment in Y Direction</i> MY (kN.m)	<i>Max. Interstory Drift Ratio</i>	<i>Max. Isolator Displacement</i> (cm)		
FEMA-273	TIME HISTORY	Z1	2.09	6156	6885	59413	53405	0.0070	30.8	NO NEED TO SCALE
		Z2	2.09	6156	6885	59413	53405	0.0070	30.8	
		Z3	2.09	8384	9377	80921	72738	0.0095	41.9	RESULTS ARE SCALED
		Z4	2.09	9560	10692	92268	82938	0.0109	47.8	
	RESPONSE SPECTRUM	Z1	2.09	6868	6859	59410	59415	0.0073	30.6	RESULTS ARE SCALED
		Z2	2.09	8582	8572	74213	74225	0.0091	38.3	
		Z3	2.09	12226	12211	105702	105720	0.0129	54.5	
		Z4	2.09	13940	13923	120501	120528	0.0149	62.1	
	EQUIVALENT LATERAL	Z1	2.09	5432	5432	57081	57081	0.0062	29.0	NO NEED TO SCALE
		Z2	2.09	6790	6790	71351	71351	0.0071	33.3	
		Z3	2.09	9670	9670	101609	101609	0.0102	50.5	
		Z4	2.09	11027	11027	115867	115867	0.0124	59.0	
IBC2000	TIME HISTORY	Z1	2.09	6156	6885	59413	53405	0.0070	30.8	NO NEED TO SCALE
		Z2	2.09	6729	7525	64938	58372	0.0077	33.7	
		Z3	2.09	9585	10720	92506	83152	0.0109	48.0	RESULTS ARE SCALED
		Z4	2.09	10927	12221	105458	94794	0.0124	54.7	
	RESPONSE SPECTRUM	Z1	2.09	6043	6035	52274	52279	0.0064	26.9	RESULTS ARE SCALED
		Z2	2.09	7550	7541	65289	65301	0.0080	33.7	
		Z3	2.09	10756	10743	92995	93011	0.0114	47.9	
		Z4	2.09	12260	12245	105978	106002	0.0131	54.7	
	EQUIVALENT LATERAL	Z1	2.09	5432	5432	57081	57081	0.0062	29.0	NO NEED TO SCALE
		Z2	2.09	6790	6790	71351	71351	0.0071	33.3	
		Z3	2.09	9670	9670	101609	101609	0.0102	50.5	
		Z4	2.09	11027	11027	115867	115867	0.0124	59.0	

Table 5.13 Results of the analyses for Type-III

		<i>T</i> (sec)	<i>Base Shear in X Direction</i> VX (kN)	<i>Base Shear in Y Direction</i> VY (kN)	<i>Base Moment in X Direction</i> MX (kN.m)	<i>Base Moment in Y Direction</i> MY (kN.m)	<i>Max. Interstory Drift Ratio</i>	<i>Max. Isolator Displacement</i> (cm)		
FEMA-273	TIME HISTORY	Z1	2.73	8040	8974	119026	106886	0.0094	40.3	NO NEED TO SCALE
		Z2	2.73	8040	8974	119026	106886	0.0094	40.3	
		Z3	2.73	10949	12222	160852	145580	0.0128	54.8	RESULTS ARE SCALED
		Z4	2.73	12486	13936	184847	165994	0.0146	62.5	
	RESPONSE SPECTRUM	Z1	2.73	8970	8931	118865	118915	0.0098	40.0	RESULTS ARE SCALED
		Z2	2.73	11223	11173	148676	148718	0.0122	50.0	
		Z3	2.73	15967	15893	211244	211414	0.0174	71.2	
		Z4	2.73	18225	18142	240976	241210	0.0198	81.2	
	EQUIVALENT LATERAL	Z1	2.73	7101	7101	114149	114149	0.0083	37.9	NO NEED TO SCALE
		Z2	2.73	8877	8877	142686	142686	0.0095	43.2	
		Z3	2.73	12642	12642	203196	203196	0.0137	66.0	
		Z4	2.73	14416	14416	231709	231709	0.0166	77.1	
IBC2000	TIME HISTORY	Z1	2.73	8040	8974	119026	106886	0.0094	40.3	NO NEED TO SCALE
		Z2	2.73	8430	9001	121012	116057	0.0103	44.5	
		Z3	2.73	12007	12821	171837	164800	0.0145	63.2	RESULTS ARE SCALED
		Z4	2.73	13688	14616	196118	188086	0.0165	71.9	
	RESPONSE SPECTRUM	Z1	2.73	6990	6959	92626	92666	0.0076	31.1	RESULTS ARE SCALED
		Z2	2.73	8748	8708	115883	115916	0.0095	38.9	
		Z3	2.73	12441	12383	164591	164723	0.0135	55.5	
		Z4	2.73	15137	15068	200147	200341	0.0165	63.2	
	EQUIVALENT LATERAL	Z1	2.73	7101	7101	114149	114149	0.0083	37.9	NO NEED TO SCALE
		Z2	2.73	8877	8877	142686	142686	0.0095	43.2	
		Z3	2.73	12642	12642	203196	203196	0.0137	66.0	
		Z4	2.73	14416	14416	231709	231709	0.0166	77.1	

Table 5.14 Comparison Table for Type-II
(Results are scaled according to IBC2000 Time History Analysis)

		T (sec)	Base Shear in X Direction V _x (kN)	Base Shear in Y Direction V _y (kN)	Base Moment in X Direction M _x (kN.m)	Base Moment in Y Direction M _y (kN.m)	Max. Interstory Drift Ratio	Max. Isolator Displacement (cm)	
FEMA-273	TIME HISTORY	Z1	1.00	1.00	1.00	1.00	1.00	1.00	NO NEED TO SCALE
		Z2	1.00	0.91	0.91	0.91	0.91	0.91	
		Z3	1.00	0.87	0.87	0.87	0.87	0.87	RESULTS ARE SCALED
		Z4	1.00	0.87	0.87	0.87	0.87	0.87	
	RESPONSE SPECTRUM	Z1	1.00	1.12	1.00	1.00	1.11	1.04	RESULTS ARE SCALED
		Z2	1.00	1.28	1.14	1.14	1.27	1.19	
		Z3	1.00	1.28	1.14	1.14	1.27	1.18	
		Z4	1.00	1.28	1.14	1.14	1.27	1.20	
	EQUIVALENT LATERAL	Z1	1.00	0.88	0.79	0.96	1.07	0.89	NO NEED TO SCALE
		Z2	1.00	1.01	0.90	1.10	1.22	0.93	
		Z3	1.00	1.01	0.90	1.10	1.22	0.94	
		Z4	1.00	1.01	0.90	1.10	1.22	1.00	
IBC2000	TIME HISTORY	Z1	1.00	1.00	1.00	1.00	1.00	1.00	NO NEED TO SCALE
		Z2	1.00	1.00	1.00	1.00	1.00	1.00	
		Z3	1.00	1.00	1.00	1.00	1.00	1.00	RESULTS ARE SCALED
		Z4	1.00	1.00	1.00	1.00	1.00	1.00	
	RESPONSE SPECTRUM	Z1	1.00	0.98	0.88	0.88	0.98	0.91	RESULTS ARE SCALED
		Z2	1.00	1.12	1.00	1.01	1.12	1.05	
		Z3	1.00	1.12	1.00	1.01	1.12	1.05	
		Z4	1.00	1.12	1.00	1.00	1.12	1.05	
	EQUIVALENT LATERAL	Z1	1.00	0.88	0.79	0.96	1.07	0.89	NO NEED TO SCALE
		Z2	1.00	1.01	0.90	1.10	1.22	0.93	
		Z3	1.00	1.01	0.90	1.10	1.22	0.94	
		Z4	1.00	1.01	0.90	1.10	1.22	1.00	

In both IBC2000 and FEMA-273, it is mentioned that if three time history data sets are used in the analysis of a structure, the maximum value of each response parameter should be used to determine design acceptability; where as if seven or more time history data sets are employed, the average value of each response parameter is permitted to be used. As mentioned in Section 3.3.3, seven different ground motion data sets are used in the time history analysis and average of each design parameter is presented in Table 5.11. When the results of each time history analysis, given in Table 5.13, are examined, one would figure out that Coyote Lake ground motion displaces the isolators only 3.7cm. It means that the ground motion does not impact the model structure extensively. This outcome is the expected result of low magnitude of Coyote Lake earthquake, $M_w = 5.7$, compared to other earthquake data.

Table 5.15 Results of time history analysis for each earthquake record, Type-II

		Site Condition	Base Shear in X Direction V_x (kN)	Base Shear in Y Direction V_y (kN)	Base Moment in X Direction M_x (kN.m)	Base Moment in Y Direction M_y (kN.m)	Max. Interstorey Drift Ratio	Max. Isolator Displacement (cm)	Shear Strain (%)
FAR FAULT	DÜZCE	Soft Soil	11671	11616	99533	100423	0.0110	52.0	260
	IMPERIAL VALLEY	Soft Soil	11123	11115	96341	96020	0.0125	49.6	248
	LANDERS	Rock	3993	3958	34443	34761	0.0040	17.8	89
	LOMA PRIETA	Hard Soil	5586	5577	48423	48205	0.0057	24.9	124
NEAR FAULT	COYOTE LAKE	Rock	836	838	7346	7256	0.0008	3.7	19
	KOCAELI	Rock	6578	11616	99533	56885	0.0110	51.8	259
	SUPERSTITT HILLS	Rock	3309	3475	30275	30284	0.0042	15.5	78
Average			6156	6885	59413	53405	0.0070	30.8	154

The parameters used for design purposes show great modification depending upon the used scaling factor. The following figures are prepared to be able to comprehend this effect. The relevant comments, in Section 5.3, on comparison of IBC2000 and FEMA-273 are made in the light of following figures.

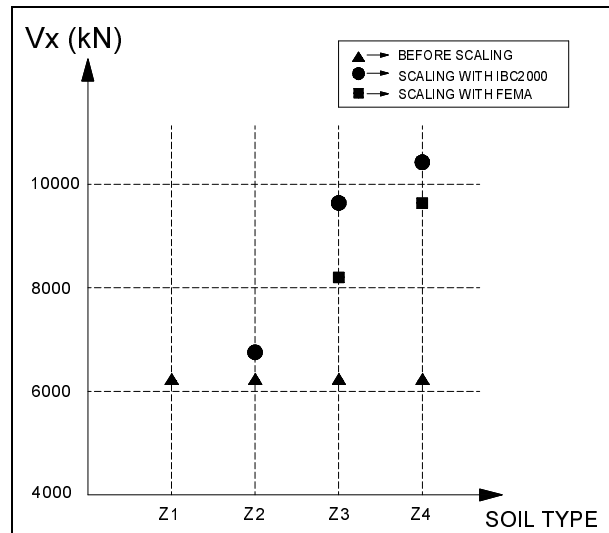


Figure 5.1 Base shear in X direction, (Type-II, time history analysis)

Base shear values in X direction as a function of soil types are given above in Figure 5.1. Before scaling and after scaling values are presented. As it is seen for soil type Z1 there is no need of scaling for both methods. For Z2 type only, scaling according to IBC2000 is needed. The significance of scaling is increased as the soil becomes softer.

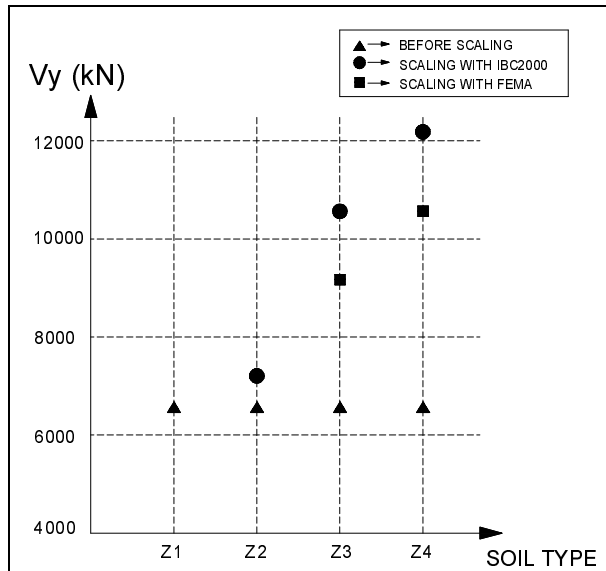


Figure 5.2 Base shear in Y direction, (Type-II, time history analysis)

Base shear values in Y direction as a function of soil types are given above in Figure 5.2. The similar behavior, described above for base shear in X direction, is also seen for base shear in Y direction.

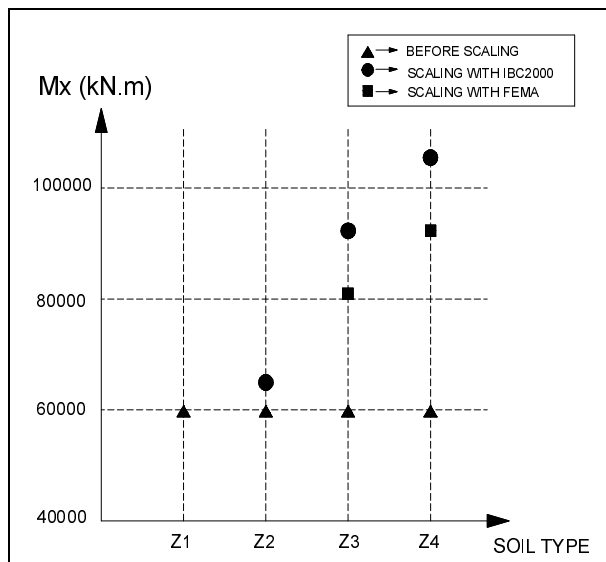


Figure 5.3 Base moment in X direction, (Type-II, time history analysis)

Base moment values in X direction as a function of soil types are given above in Figure 5.3. Before scaling and after scaling values are presented. As it is seen for soil type Z1 there is no need of scaling for both methods. For Z2 type only, scaling according to IBC2000 is needed. The significance of scaling is increased as the soil becomes softer.

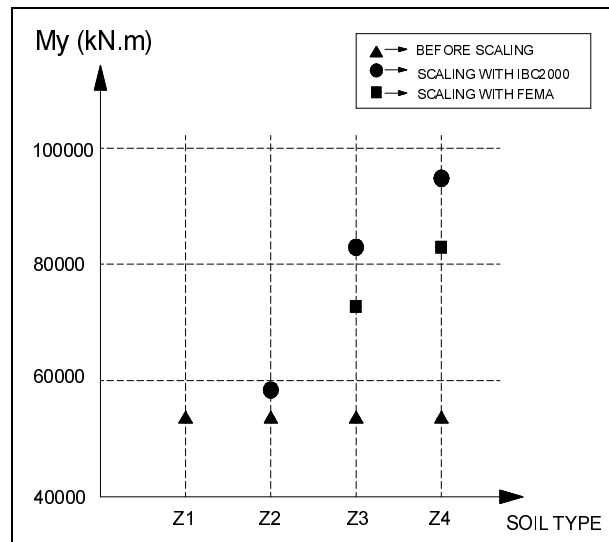


Figure 5.4 Base moment in Y direction, (Type-II, time history analysis)

Base moment values in Y direction as a function of soil types are given above in Figure 5.4. . The similar behavior, described above for base moment in X direction, is also seen for base moment in Y direction.

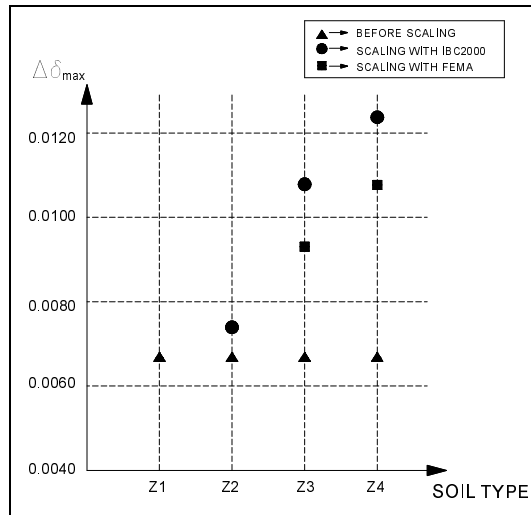


Figure 5.5 Maximum interstory drift ratio, (Type-II, time history analysis)

Maximum interstory drift ratios as a function of soil types are given above in Figure 5.5. Before scaling and after scaling values are presented. As it is seen for soil type Z1 there is no need of scaling for both methods. For Z2 type only, scaling according to IBC2000 is needed. The significance of scaling is increased as the soil becomes softer.

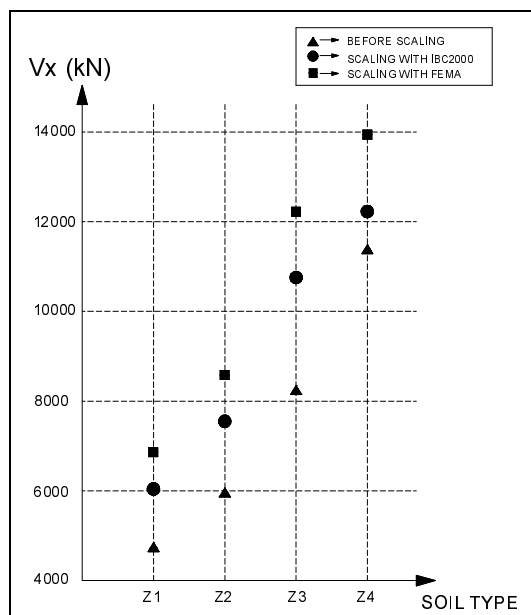


Figure 5.6 Base shear in X direction, (Type-II, response spectrum analysis)

Base shear values in X direction as a function of soil types are given above in Figure 5.6. Before scaling and after scaling values are presented. As it is seen, the results are scaled according to both IBC2000 and FEMA-273 for all of the soil types. The significance of scaling does not affected by soil type except that it is decreased for soil type Z4.

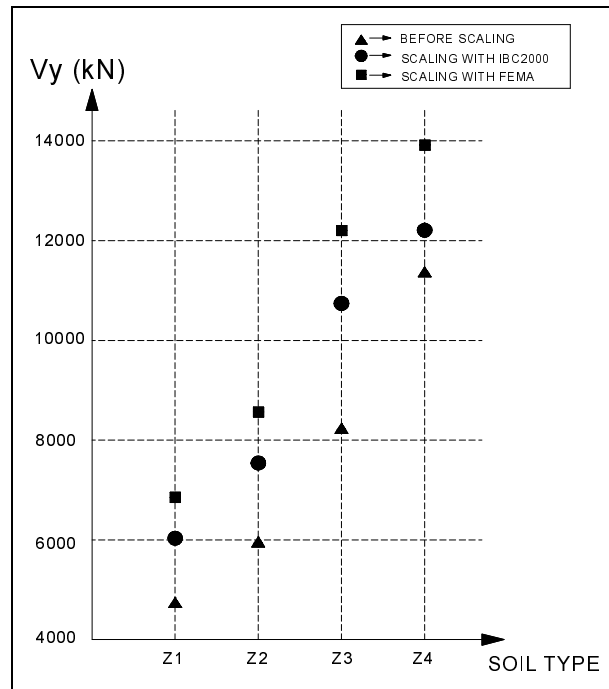


Figure 5.7 Base shear in Y direction, (Type-II, response spectrum analysis)

Base shear values in Y direction as a function of soil types are given above in Figure 5.7. . The similar behavior, described above for base shear in X direction, is also seen for base shear in Y direction.

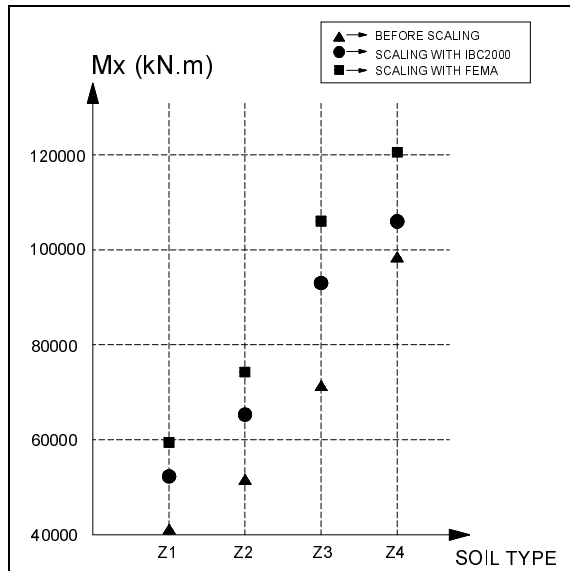


Figure 5.8 Base moment in X direction, (Type-II, response spectrum analysis)

Base moment values in X direction as a function of soil types are given above in Figure 5.8. Before scaling and after scaling values are presented. As it is seen, the results are scaled according to both IBC2000 and FEMA-273 for all of the soil types. The significance of scaling does not affected by soil type except that it is decreased for soil type Z4.

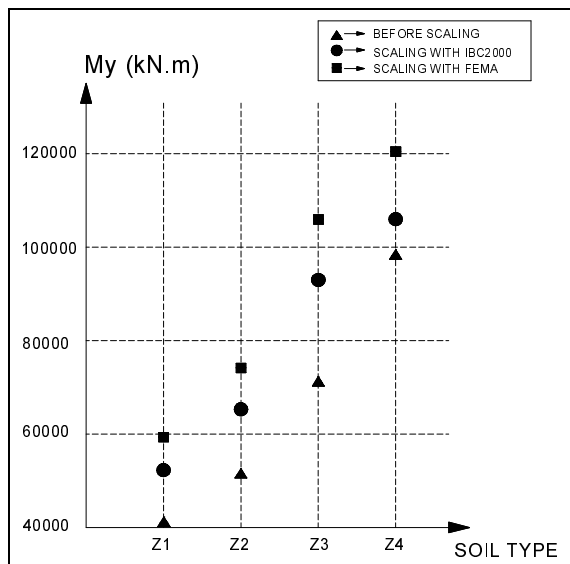


Figure 5.9 Base moment in Y direction, (Type-II, response spectrum analysis)

Base moment values in Y direction as a function of soil types are given above in Figure 5.9. . The similar behavior, described above for base moment in X direction, is also seen for base moment in Y direction.

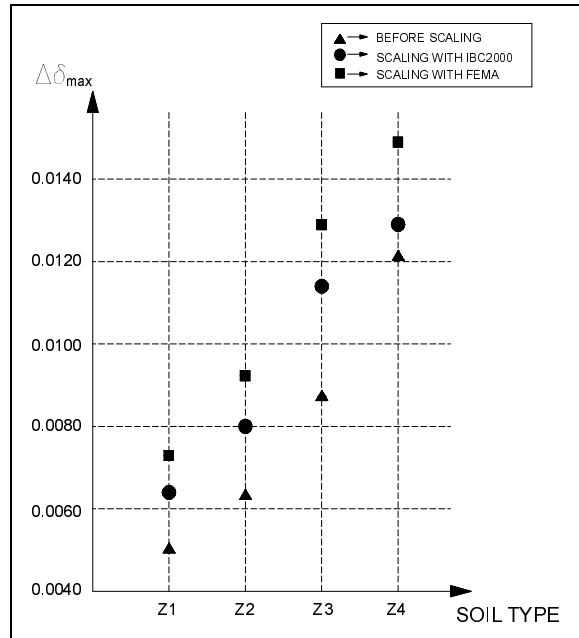


Figure 5.10 Maximum interstory drift ratio, (Type-II, response spectrum analysis)

Maximum interstory drift ratios as a function of soil types are given above in Figure 5.10. Before scaling and after scaling values are presented. As it is seen, the results are scaled according to both IBC2000 and FEMA-273 for all of the soil types. The significance of scaling does not affected by soil type except that it is decreased for soil type Z4.

5.2 Analysis of the Base Isolated Non-symmetrical Building

To identify the effect of “scaling” phenomenon mentioned in FEMA-273 & IBC2000 and make a comparison between these two codes from the “scaling” point of view, building Type-IV, introduced in Section 3.2.4, is analyzed. The high damping rubber bearings, HDR, designed in Section 4.1 are used for the isolation of the buildings. Static equivalent lateral force, response spectrum and time history analyses, described in Sections 3.3.1, 3.3.2 and 3.3.3, are carried out on the model building which typifies the class of non-symmetrical structure that is encountered in design. The analyses of the isolated buildings are done for each soil type that is given in the Turkish Seismic Code (Z1, Z2, Z3, and Z4).

5.2.1 Scaling of the Results

The results of the analyses are scaled according to both FEMA-273 and IBC2000 as mentioned in Section 3.4. The detailed calculation of scaling factors for each analysis method is given below.

5.2.1.1 Scaling for Static Equivalent Lateral Force Procedure

The limits of scaling mentioned in FEMA-273 and IBC2000 for static equivalent lateral force procedure are the same except that an additional limit is also defined in IBC2000: “The base shear must be greater than the lateral seismic force required for a fixed-base structure of the same weight and a period equal to the isolated period”.

Building Type-IV is analyzed with static equivalent lateral force procedure and the results of the analysis are scaled according to the mentioned limit. For the calculation of the lateral seismic force, V_T , the procedure described in Turkish Seismic Code is used.

$$A_0 = 0.40$$

$$I = 1.4$$

$$R = 8 \text{ (Seismic load reduction factor for non-isolated building)}$$

$$W_T = 15065 \text{ kN}$$

$$T_D = 1.95 \text{ sec.}$$

Table 5.16 Calculation of scaling factor for Type-IV according to IBC2000

	S(T)	A(T) (Equation 5.2)	V_T (kN) (Equation 5.1)	V_S (kN) (Equation 3.5)	Scaling Factor
Z1	0.559	0.313	590	3985	no need to scale
Z2	0.704	0.394	743	4977	no need to scale
Z3	0.974	0.545	1028	7084	no need to scale
Z4	1.347	0.754	1421	8094	no need to scale

5.2.1.2 Scaling for Response Spectrum Analysis

Building Type IV is analyzed with response spectrum analysis and the results of the analysis are scaled according to both FEMA-273 and IBC2000. To be comprehensible, the parameters needed for the calculation of scaling factors are given below. The damping coefficient, B_D , is taken as 1.38 for the calculations since the HDR, bearings designed in Section 4.1, are used for the isolation. As a result of the modal analysis the fixed based, T , and isolated periods, T_D , of the building are determined as:

Table 5.17 Fixed and isolated periods

	Type-IV
T (sec.)	0.43
T_D (sec.)	1.95

Scaling according to IBC2000:

When the IBC2000 is considered, the design displacement determined by response spectrum analysis, $D_{analysis}$, must be greater than 90% of D_{TD} , as specified in Equation 3.4. On the other hand, the design base shear force on the structure above the isolation system must be greater than V_S as prescribed by Equation 3.5. Otherwise, all response parameters, including component actions and deformations, must be adjusted proportionally upward.

When the results of the analyses are examined, it is seen that the first scaling limit, $D_{analysis} > 0.9 \times D_{TD}$, is more critical than the second one and results in greater scaling factors. Therefore, displacement dependent scaling limit is used in the scaling factor calculations.

Table 5.18 Calculation of scaling factor for Type-IV according to IBC2000

	S_{D1}	D_D (cm) (Equation 3.1)	$D_{D'}$ (cm) (Equation 3.7)	$0,9 * D_{TD'}$ (cm) (Equation 3.4)	$D_{analysis}$ (cm)	Scaling Factor
Z1	0.64	22.50	22.00	25.15	20.73	1.213
Z2	0.80	28.10	27.40	31.32	26.10	1.200
Z3	1.14	40.00	39.10	44.69	36.08	1.239
Z4	1.30	45.70	44.60	50.98	49.91	1.021

Scaling according to FEMA-273:

When the FEMA-273 is considered, the design displacement determined by response spectrum analysis, $D_{analysis}$, must be greater than the value of D_{TD} prescribed by Equation 3.4. Otherwise, all response parameters, including component actions and deformations, must be adjusted upward proportionally to the D_{TD} value and used for design.

Table 5.19 Calculation of scaling factor for Type-IV according to FEMA-273

	S_{D1}	D_D (cm) (Equation 3.1)	D_{TD} (cm) (Equation 3.4)	$D_{analysis}$ (cm)	Scaling Factor
Z1	0.64	22.50	28.58	20.73	1.378
Z2	0.80	28.10	35.69	26.10	1.367
Z3	1.14	40.00	50.80	36.08	1.408
Z4	1.30	45.70	58.04	49.91	1.163

5.2.1.3 Scaling for Time History Analysis

Building Type IV is analyzed with time history analysis and the results of the analysis are scaled according to both FEMA-273 and IBC2000. The parameters needed for the calculation of scaling factors are given below. The damping coefficient, B_D , is taken as 1.38 for the calculations since the HDR, bearings designed in Section 4.1, are used for the analysis. The fixed based, T , and isolated periods, T_D , of the building are as given in Table 5.15.

Scaling according to IBC2000

The displacement dependent scaling limit for time history analysis is same with the one given for response spectrum analysis. However, the design base shear force on the structure above the isolation system must be greater than 80% of V_S as prescribed by Equation 3.5. Otherwise, all response parameters, including component actions and deformations, must be adjusted proportionally upward.

When the results of the analyses are examined, it is seen that the first scaling limit, $D_{analysis} > 0.9 \times D_{TD}$, is more critical than the second one and results in greater scaling factors. Therefore, it is used in the scaling factor calculations.

Table 5.20 Calculation of scaling factor for Type-IV according to IBC2000

	S_{D1}	D_D (cm) (Equation 3.1)	$D_{D'}$ (cm) (Equation 3.7)	$0,9 * D_{TD'}$ (cm) (Equation 3.4)	$D_{analysis}$ (cm)	Scaling Factor
Z1	0.64	22.50	22.00	25.15	30.70	no need to scale
Z2	0.80	28.10	27.40	31.32	30.70	1.020
Z3	1.14	40.00	39.10	44.69	30.70	1.456
Z4	1.30	45.70	44.60	50.98	30.70	1.661

Scaling according to FEMA-273

When the FEMA-273 is considered, the design displacement determined by time history analysis, $D_{analysis}$, must be greater than the value of $D_{D'}$ prescribed by Equation 3.7. Otherwise, all response parameters, including component actions and deformations, must be adjusted upward proportionally to the $D_{D'}$ value and used for design.

Table 5.21 Calculation of scaling factor for Type-IV according to FEMA-273

	S_{D1}	D_D (cm) (Equation 3.1)	$D_{D'}$ (cm) (Equation 3.7)	$D_{analysis}$ (cm)	Scaling Factor
Z1	0.64	22.50	22.00	30.70	no need to scale
Z2	0.80	28.10	27.40	30.70	no need to scale
Z3	1.14	40.00	39.10	30.70	1.27
Z4	1.30	45.70	44.60	30.70	1.45

5.2.2 Results of the Analyses

The results of the analyses of building Type-IV, representing the typical non-symmetrical structure, are given in Table 5.20 below; also in order to be able to compare different analysis methods a comparison table, Table 5.21, is prepared. It can be concluded from the comparison table that response spectrum analysis, scaled according to FEMA-273 provisions, results in the most conservative design values.

Table 5.22 Results of the analyses for Type-IV

		T (sec)	Base Shear in X Direction V _x (kN)	Base Shear in Y Direction V _y (kN)	Base Moment in X Direction M _x (kN.m)	Base Moment in Y Direction M _y (kN.m)	Rotational Moment M _z (kN.m)	Max. Interstory Drift Ratio	Max. Isolator Disp. (cm)		
FEMA-273	TIME HISTORY	Z1	1.95	4485	5040	41153	36253	20350	0.0070	30.7	NO NEED TO SCALE
		Z2	1.95	4485	5040	41153	36253	20350	0.0070	30.7	
		Z3	1.95	5696	6401	52264	46041	25845	0.0089	39.0	RESULTS ARE SCALED
		Z4	1.95	6503	7308	59672	52567	29508	0.0102	44.5	
	RESPONSE SPECTRUM	Z1	1.95	4656	4627	41312	41459	19400	0.0066	28.6	RESULTS ARE SCALED
		Z2	1.95	5815	5780	51581	51768	24234	0.0082	35.7	
		Z3	1.95	8282	8231	73426	73698	34510	0.0117	50.8	
		Z4	1.95	9463	9405	83890	84201	39435	0.0134	58.0	
	EQUIVALENT LATERAL	Z1	1.95	3985	3985	43835	43835	14784	0.0055	33.4	NO NEED TO SCALE
		Z2	1.95	4977	4977	54747	54747	18465	0.0069	41.6	
		Z3	1.95	7084	7084	77924	77924	26282	0.0099	59.1	
		Z4	1.95	8094	9084	89034	89034	33702	0.0114	67.6	
IBC2000	TIME HISTORY	Z1	1.95	4485	5040	41153	36253	20350	0.0070	30.7	NO NEED TO SCALE
		Z2	1.95	4575	5141	41976	36978	20757	0.0071	31.3	RESULTS ARE SCALED
		Z3	1.95	6530	7338	59919	52784	29630	0.0102	44.7	
		Z4	1.95	7450	8371	68355	60216	33801	0.0116	51.0	
	RESPONSE SPECTRUM	Z1	1.95	4098	4073	36366	36494	17077	0.0058	25.2	
		Z2	1.95	5105	5074	45280	45444	21273	0.0072	31.3	
		Z3	1.95	7288	7243	64613	64852	30368	0.0103	44.7	
		Z4	1.95	8308	8257	73647	73920	34620	0.0117	51.0	
	EQUIVALENT LATERAL	Z1	1.95	3985	3985	43835	43835	14784	0.0055	33.4	NO NEED TO SCALE
		Z2	1.95	4977	4977	54747	54747	18465	0.0069	41.6	
		Z3	1.95	7084	7084	77924	77924	26282	0.0099	59.1	
		Z4	1.95	8094	9084	89034	89034	33702	0.0114	67.6	

Table 5.23 Comparison Table for Type-IV
(Results are scaled according to IBC2000 Time History Analysis)

		T (sec)	Base Shear in X Direction V _x (kN)	Base Shear in Y Direction V _y (kN)	Base Moment in X Direction M _x (kN.m)	Base Moment in Y Direction M _y (kN.m)	Rotational Moment M _z (kN.m)	Max. Interstory Drift Ratio	Max. Isolator Disp. (cm)	
FEMA-273	TIME HISTORY	Z1	1.00	1.00	1.00	1.00	1.00	1.00	1.00	
		Z2	1.00	0.98	0.98	0.98	0.98	0.98	0.98	
		Z3	1.00	0.87	0.87	0.87	0.87	0.87	0.87	
		Z4	1.00	0.87	0.87	0.87	0.87	0.87	0.87	
	RESPONSE SPECTRUM	Z1	1.00	1.04	0.92	1.00	1.14	0.95	0.94	0.93
		Z2	1.00	1.27	1.12	1.23	1.40	1.17	1.15	1.14
		Z3	1.00	1.27	1.12	1.23	1.40	1.16	1.15	1.14
		Z4	1.00	1.27	1.12	1.23	1.40	1.17	1.15	1.14
	EQUIVALENT LATERAL	Z1	1.00	0.89	0.79	1.07	1.21	0.73	0.79	1.09
		Z2	1.00	1.09	0.97	1.30	1.48	0.89	0.97	1.33
		Z3	1.00	1.08	0.97	1.30	1.48	0.89	0.97	1.32
		Z4	1.00	1.09	1.09	1.30	1.48	1.00	0.98	1.33
IBC2000	TIME HISTORY	Z1	1.00	1.00	1.00	1.00	1.00	1.00	1.00	
		Z2	1.00	1.00	1.00	1.00	1.00	1.00	1.00	
		Z3	1.00	1.00	1.00	1.00	1.00	1.00	1.00	
		Z4	1.00	1.00	1.00	1.00	1.00	1.00	1.00	
	RESPONSE SPECTRUM	Z1	1.00	0.91	0.81	0.88	1.01	0.84	0.83	0.82
		Z2	1.00	1.12	0.99	1.08	1.23	1.02	1.01	1.00
		Z3	1.00	1.12	0.99	1.08	1.23	1.02	1.01	1.00
		Z4	1.00	1.12	0.99	1.08	1.23	1.02	1.01	1.00
	EQUIVALENT LATERAL	Z1	1.00	0.89	0.79	1.07	1.21	0.73	0.79	1.09
		Z2	1.00	1.09	0.97	1.30	1.48	0.89	0.97	1.33
		Z3	1.00	1.08	0.97	1.30	1.48	0.89	0.97	1.32
		Z4	1.00	1.09	1.09	1.30	1.48	1.00	0.98	1.33

In both IBC2000 and FEMA-273, it is mentioned that the selected ground motion sets for time history analysis must have magnitude, fault distance and source mechanism that are equivalent to design earthquake ground motion. The results of each time history analysis are given in Table 5.12 and Table 5.22 for five-storey symmetrical, Type-II, and non-symmetrical, Type-IV, building types respectively. When the results are examined; it is clear that in addition to the magnitude, fault distance and source mechanism, also the conditions of site where earthquake data is recorded have a great influence on the results. As the soil where the ground motion data is recorded, becomes softer the response of the structure increases. Therefore when selecting a ground motion data set, site condition must be also taken into account in addition. When the results of each time history analysis, given in Table 5.22, are examined, one would figure out that Coyote Lake ground motion displaces the isolators only 4.0cm. It means that the ground motion does not impact the model structure extensively. This outcome is the expected result of low magnitude of Coyote Lake earthquake, $M_w = 5.7$, compared to other earthquake data.

Table 5.24 Results of time history analysis for each earthquake record, Type-IV

		Site Condition	Base Shear in X Direction V_x (kN)	Base Shear in Y Direction V_y (kN)	Base Moment in X Direction M_x (kN.m)	Base Moment in Y Direction M_y (kN.m)	Max. Interstory Drift Ratio	Max. Isolator Disp. (cm)	Shear Strain (%)
FAR FAULT	DÜZCE	Soft Soil	8573	8441	75537	76913	0.0102	52.8	264
	IMPERIAL VALLEY	Soft Soil	7692	7684	42263	42253	0.0121	44.8	224
	LANDERS	Rock	3863	3804	33875	34130	0.0057	22.6	113
	LOMA PRIETA	Hard Soil	3182	3254	29036	28425	0.0053	19.7	99
NEAR FAULT	COYOTE LAKE	Rock	699	693	5747	6661	0.0009	4.0	20
	KOCAELI	Rock	4399	8441	75537	39024	0.0101	52.8	264
	S. HILLS	Rock	2990	2961	26075	26368	0.0046	17.9	90
Average			4485	5040	41153	36253	0.0070	30.7	154

The following figures are prepared to be able to comprehend scaling effect. The relevant comments, in Section 5.3, on comparison of IBC2000 and FEMA-273 are made in the light of following figures.

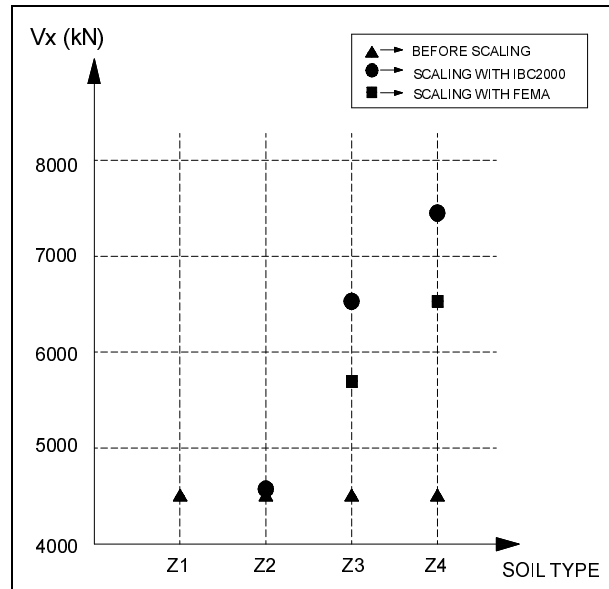


Figure 5.11 Base shear in X direction, (Type-IV, time history analysis)

Base shear values in X direction as a function of soil types are given above in Figure 5.11. Before scaling and after scaling values are presented. As it is seen for soil type Z1 there is no need of scaling for both methods. For Z2 type only, scaling according to IBC2000 is needed. The significance of scaling is increased as the soil becomes softer.

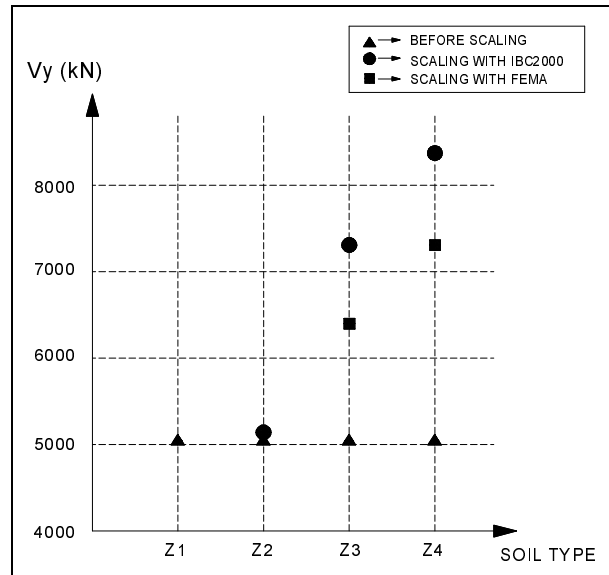


Figure 5.12 Base shear in Y direction, (Type-IV, time history analysis)

Base shear values in Y direction as a function of soil types are given above in Figure 5.12. . The similar behavior, described above for base shear in X direction, is also seen for base shear in Y direction.

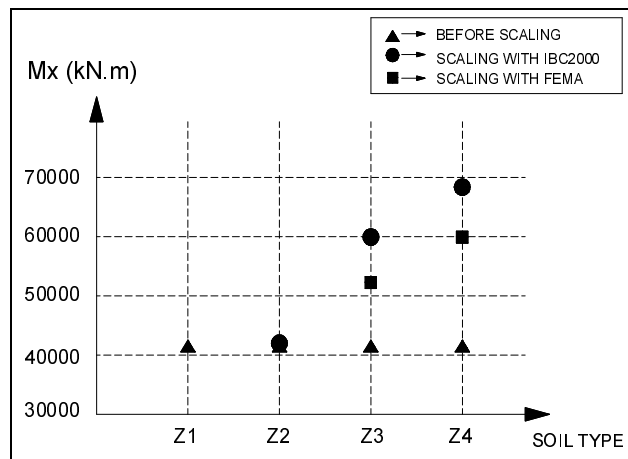


Figure 5.13 Base moment in X direction, (Type-IV, time history analysis)

Base moment values in X direction as a function of soil types are given above in Figure 5.13. Before scaling and after scaling values are presented. As it is seen for soil type Z1 there is no need of scaling for both methods. For Z2 type only, scaling according to IBC2000 is needed. The significance of scaling is increased as the soil becomes softer.

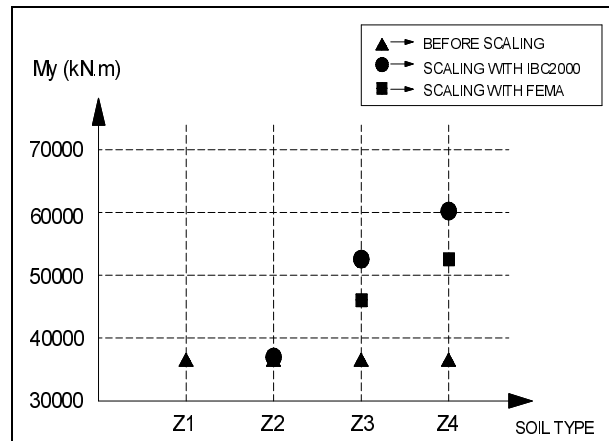


Figure 5.14 Base moment in Y direction, (Type-IV, time history analysis)

Base moment values in Y direction as a function of soil types are given above in Figure 5.14. . The similar behavior, described above for base moment in X direction, is also seen for base moment in Y direction.

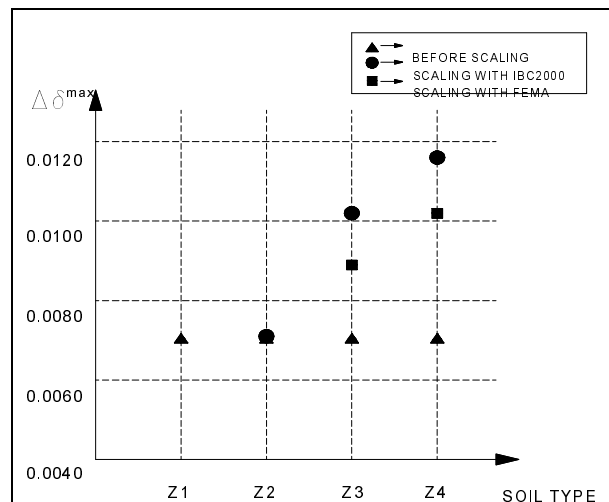


Figure 5.15 Maximum interstory drift ratio, (Type-IV, time history analysis)

Maximum interstory drift ratios as a function of soil types are given above in Figure 5.15. Before scaling and after scaling values are presented. As it is seen for soil type Z1 there is no need of scaling for both methods. For Z2 type only, scaling according to IBC2000 is needed. The significance of scaling is increased as the soil becomes softer.

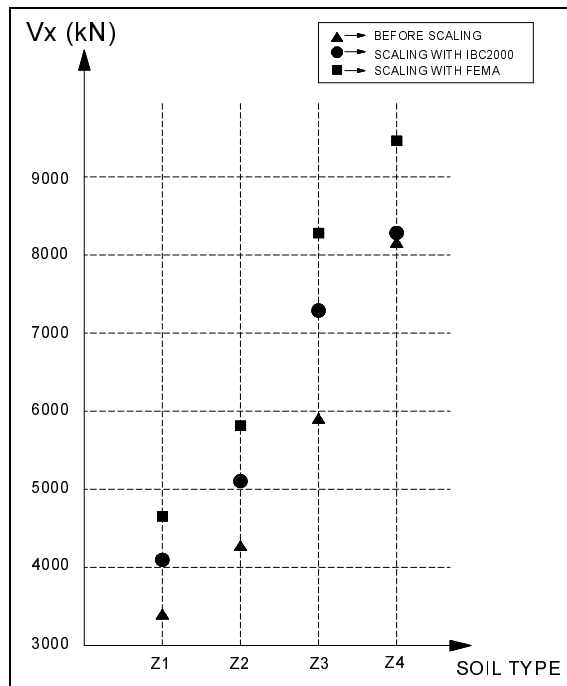


Figure 5.16 Base shear in X direction, (Type-IV, response spectrum analysis)

Base shear values in X direction as a function of soil types are given above in Figure 5.16. Before scaling and after scaling values are presented. As it is seen, the results are scaled according to both IBC2000 and FEMA-273 for all of the soil types. The significance of scaling does not affected by soil type except that it is decreased for soil type Z4.

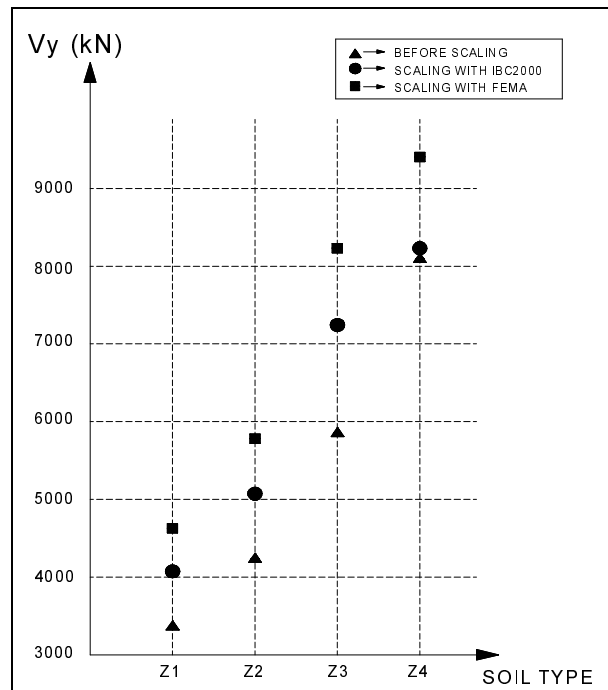


Figure 5.17 Base shear in Y direction, (Type-IV, response spectrum analysis)

Base shear values in Y direction as a function of soil types are given above in Figure 5.17. . The similar behavior, described above for base shear in X direction, is also seen for base shear in Y direction.

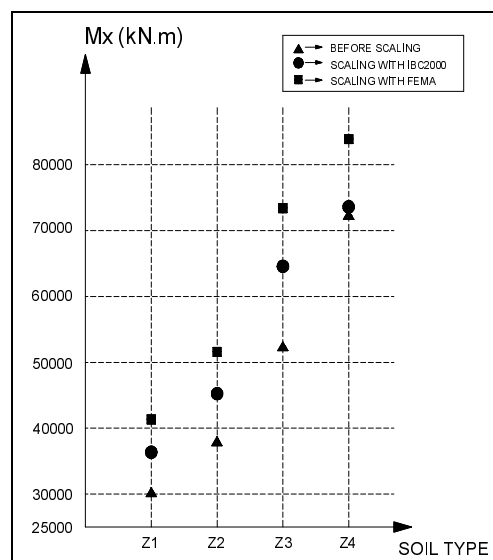


Figure 5.18 Base moment in X direction, (Type-IV, response spectrum analysis)

Base moment values in X direction as a function of soil types are given above in Figure 5.18. Before scaling and after scaling values are presented. As it is seen, the results are scaled according to both IBC2000 and FEMA-273 for all of the soil types. The significance of scaling does not affected by soil type except that it is decreased for soil type Z4.

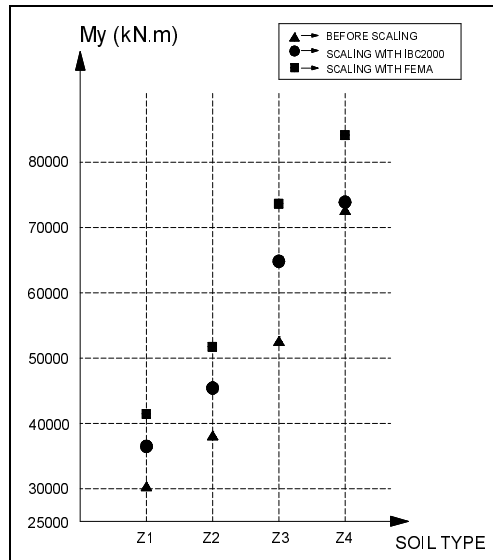


Figure 5.19 Base moment in Y direction, (Type-IV, response spectrum analysis)

Base moment values in Y direction as a function of soil types are given above in Figure 5.19. . The similar behavior, described above for base moment in X direction, is also seen for base moment in Y direction.

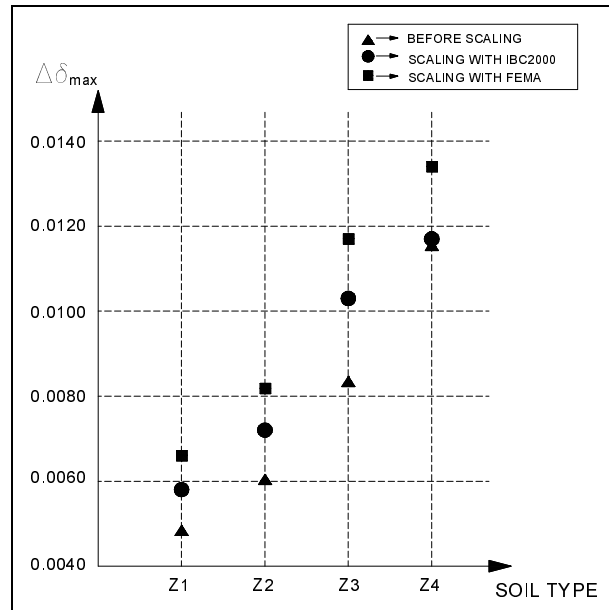


Figure 5.20 Maximum interstory drift ratio, (Type-IV, response spectrum analysis)

Maximum interstory drift ratios as a function of soil types are given above in Figure 5.20. Before scaling and after scaling values are presented. As it is seen, the results are scaled according to both IBC2000 and FEMA-273 for all of the soil types. The significance of scaling does not affected by soil type except that it is decreased for soil type Z4.

5.3 Comparison of FEMA-273 and IBC2000

When the results of the analyses, which are given in Figures 5.1 through 5.20, are studied; one would figure out that the codes FEMA-273 and IBC2000 give different

results for the same analysis method. The reason for this variation mainly depends on the difference in the accepted provisions for scaling of the analysis results. Below, the comparison of the scaling provisions, recommended in FEMA-273 and IBC2000, is done for each method used in the analysis.

5.3.1 Equivalent Lateral Load Analysis

It can be seen from the Tables 5.11 & 5.20 that IBC2000 and FEMA-273 gives identical results since the results are not needed to be scaled.

5.3.2 Response Spectrum Analysis

FEMA-273 gives more critical values for the design when response spectrum analysis is considered. The reason depends on the difference between the accepted scaling thresholds, which are defined in FEMA-273 and IBC2000.

While IBC2000 takes $0.9 \times D_{TD}$ as limit for scaling, FEMA-273 takes D_{TD} . If the equation for D_{TD} , Equation 3.7, is examined; it is realized that the inequality of “ $0.9 \times D_{TD} < D_{TD}$ ” is always valid, Therefore it is concluded that FEMA-273 is more conservative than IBC2000 when response spectrum analysis is concerned.

The scaling factors for response spectrum analyses are given in Tables 5.3-8, 5.16-17. When these tables are examined, it is realized that the scaling factors for each soil type are nearly constant, very close to each other, and do not fluctuate much for different soil types except soil type Z4. Actually, this is the expected trend since the effect of site condition on the scaling factor is already taken into account by assigning different spectrum functions for each soil type.

In FEMA-273 and IBC2000 site classes are categorized into six different groups as A, B, C, D, E and F. On the other hand, in Turkish Seismic Code site classes are grouped as Z1, Z2, Z3 and Z4. Although these groups do not match with each other exactly, for the determination of scaling factors, it is assumed that A stands for Z1, B stands for Z2, C stands for Z3 and D stands for Z4. The decrease in the scaling factor for soil type Z4 when compared with Z1, Z2 and Z3 basically results from this assumption. Because, Z4 is assumed to be identical with site class D for the analyses, however it represents weaker soil conditions and stands for somewhere between site

classes D, E and F. Consequently, scaling factor Z4 decreases when compared with Z1, Z2 and Z3.

5.3.3 Time History Analysis

The scaling limits for the time history analysis are:

$$D_{\text{analysis}} > D_{D'} \quad (\text{FEMA-273})$$

$$D_{\text{analysis}} > 0.9 \times D_{TD'} \quad (\text{IBC2000})$$

Which one of these limits is more conservative? In order to answer this question the applied earthquake direction must be checked.

When the Earthquake is applied in Short Direction:

If the following inequality is correct then IBC2000 is more conservative.

$$D_{D'} < (0.9 \times D_{TD'})$$

$$D_{D'} < 0.9 * D_{D'} \left[1 + y \left(\frac{12e}{b^2 + d^2} \right) \right]$$

$$1.10 < \left[1 + y \left(\frac{12e}{b^2 + d^2} \right) \right] \quad \text{where;}$$

$$b > d$$

$$e = 0.05 * b \quad (5\% \text{ min. eccentricity})$$

$$y = b/2$$

$$1.10 < \left[1 + \frac{b}{2} * \frac{(12 * 0.05 * b)}{(b^2 + d^2)} \right] = \left[1 + \frac{(0.3 * b^2)}{(b^2 + d^2)} \right]$$

$$\frac{1}{3} < \frac{b^2}{(b^2 + d^2)}$$

$$d^2 < 2 * b^2$$

This inequality is always valid since $b > d$. Therefore, the expression of $D_{D'} < (0.9 \times D_{TD'})$ is always true when earthquake is assumed to apply in short direction.

When the Earthquake is applied in Long Direction:

If the following inequality is correct then IBC2000 is more conservative.

$$D_{D'} < (0.9 \times D_{TD'})$$

$$D_{D'} < 0.9 * D_{D'} \left[1 + y \left(\frac{12e}{b^2 + d^2} \right) \right]$$

$$1.10 < \left[1 + y \left(\frac{12e}{b^2 + d^2} \right) \right] \quad \text{where;}$$

$$b > d$$

$$e = 0.05 * d \text{ (5\% min. eccentricity)}$$

$$y = d/2$$

$$1.10 < \left[1 + \frac{d}{2} * \frac{(12 * 0.05 * d)}{(b^2 + d^2)} \right] = \left[1 + \frac{(0.3 * d^2)}{(b^2 + d^2)} \right]$$

$$\frac{1}{3} < \frac{d^2}{(b^2 + d^2)}$$

$$b^2 < 2 * d^2$$

It can be commented that for time history analysis IBC2000 is more conservative when $\sqrt{2} d > b > d$. So it might seem that conservativeness of IBC2000 depends on the plan dimensions of the isolated building. However, IBC2000 states that D_{TD} can not be less than 1.1 times D_D . So;

$$1.10 < \left[1 + y \left(\frac{12e}{b^2 + d^2} \right) \right]$$

is always true no matter what the plan dimensions are. Then IBC2000 is always more conservative than FEMA-273 when time history analysis is concerned.

The scaling factors for time history analyses are given in Tables 5.9-10 and 5.18-19. When these tables are examined, it is seen that the scaling factor increases as the site condition worsen.

CHAPTER 6

CONCLUSION

In this study, the design of seismic isolation systems is explained and the influence of base isolation on the response of structure is examined in details. Various types of isolators are introduced and one of the most commonly used type, high damping rubber bearing, is used in the case studies. Both alternatives of modeling an isolator for design purposes, linear and bi-linear, are discussed; also advantages and disadvantages of them are stated. The analyses of isolated buildings, symmetrical and non-symmetrical in plan, are performed according to the related chapters of the design codes FEMA and IBC2000. According to these analyses, the codes are compared for each type of analysis method.

In the light of the results obtained from the case studies, the following conclusions can be stated:

- The assumed equivalent linear model of isolators which is accepted by the FEMA and IBC2000 design codes; underestimates the peak superstructure acceleration and overestimates the bearing displacement when compared to the bilinear model.
- For the bilinear model isolators with the increase in isolator yield displacement, D_y , the bearing displacement also increases.

- When time history analysis is used, the site condition where earthquake data is recorded has a great influence on the design parameters of the structure. That is as the soil becomes softer, the response of the structure increases. Therefore the selected ground motion data sets for time history analysis must have been recorded on similar soil condition with the site where the structure is located. It means that site condition must be also taken into account in addition to the mentioned parameters in IBC2000 and FEMA (fault distance, magnitude and source mechanism type).

- When compared with IBC2000, FEMA gives more critical values for the design if response spectrum analysis is used. The reason depends on the difference between the accepted scaling limits in FEMA and IBC2000.

- When compared with FEMA, IBC2000 gives more critical values for the design if time history analysis is used. The reason depends on the difference between the accepted scaling limits in FEMA and IBC2000.

- The scaling factor for response spectrum analysis does not change for different site conditions except for soil type Z4. The decrease in the scaling factor for soil type Z4 when compared with Z1, Z2 and Z3 basically results from the differences between the defined site conditions in IBC2000, FEMA and Turkish Seismic Code.

- The scaling factor for time history analyses increases as the site condition worsen.

REFERENCES

- [1] Farzad Naeim, James M. Kelly, “Design of Seismic Isolated Structures from Theory to Practice”, John Wiley & Sons Inc., USA, (1999)
- [2] R. Ivan Skinner, William H. Robinson, Graeme H. McVerry, “An Introduction to Seismic Isolation”, John Wiley & Sons Ltd., England, (1993)
- [3] Semih S. Tezcan, Aykut Erkal, “Seismic Base Isolation and Energy Absorbing Devices”, Higher Education Foundation, İstanbul, (2002)
- [4] Semih S. Tezcan, Serra Cimilli, “Seismic Base Isolation”, Higher Education Foundation, İstanbul, (2002)
- [5] Michael Constantinou, Hasan Karataş, “Sismik İzolasyon Yöntemiyle Binaların Depremden Korunması, İnşaat Mühendislerine Sertifika Programı Ders Notları”, İstanbul Kültür University, İstanbul, (2003)
- [6] Anıl K. Chopra, “Dynamics of Structures Theory and Applications to Earthquake Engineering”, Prentice-Hall Inc., New Jersey, (1995)
- [7] Anıl K. Chopra, “Solutions Manual and Transparency Master Dynamics of Structures Theory and Applications to Earthquake Engineering”, Prentice-Hall Inc., USA, (2001)
- [8] _____, “Specification for Structures to be Built in Disaster Areas”, Afet İşleri Genel Müdürlüğü, Ankara, (1998)

- [9] _____, “Uniform Building Code”, International Conference of Building Officials, California, (1997)
- [10] _____, “Uniform Building Code Procedures for Seismically Isolated Buildings”, Dynamic Isolation Systems Inc., USA, (1993)
- [11] _____, “International Building Code”, International Code Council Inc., USA, (2000)
- [12] Günay Özmen, Engin Orakdöğen, Kutlu Darılmaz, “Örneklerle Sap 2000-V8”, Birsen Yayınevi, İstanbul, (2004)
- [13] Sap2000n “Analysis References Volume 1”, Computers and Structures Inc., California, (1997)
- [14] Sap2000n “Analysis References Volume 2”, Computers and Structures Inc., California, (1997)
- [15] Sap2000n “Verification Manual”, Computers and Structures Inc., California, (1997)
- [16] American Society of Civil Engineers, “Prestandard and Commentary for the Seismic Rehabilitation of Buildings, FEMA Publication-356”, Federal Emergency Management Agency, Washington D.C., (2000)
- [17] Applied Technology Council, “NEHRP Guidelines for the Seismic Rehabilitation of Buildings, FEMA Publication-273”, Building Seismic Safety Council, Washington D.C., (1997)
- [18] Applied Technology Council, “Seismic Evaluation and Retrofit of Concrete Buildings, ATC-40 Volume-1”, Seismic Safety Commission, California, (1996)
- [19] Applied Technology Council, “Seismic Evaluation and Retrofit of Concrete Buildings, ATC-40 Volume-2”, Seismic Safety Commission, California, (1996)

- [20] Vasant A. Matsagar, R. S. Jangid, “Influence of Isolator Characteristics on the Response of Base-Isolated Structures”, Department of Civil Engineering, Indian Institute of Technology, Elsevier Ltd., Bombay, (2004)
- [21] Alessandro Baratta, Ileana Corbi, “Optimal Design of Base-Isolators in Multi-storey Buildings”, Department of ‘Scienza delle Costruzioni’, University of Naples, Elsevier Ltd., Civil-Comp Ltd., Italy, (2004)
- [22] W. H. Robinson, “Seismic Isolation of Civil Buildings in New Zealand”, John Wiley & Sons Ltd., New Zealand, (2000)
- [23] Fu Lin Zhou, “Seismic Isolation of Civil Buildings in the People’s Republic of China”, Guangzhou University, John Wiley & Sons Ltd., China, (2001)
- [24] Applied Technology Council, “NEHRP Commentary on the Guidelines for the Seismic Rehabilitation of Buildings, FEMA Publication-274”, Building Seismic Safety Council, Washington D.C., (1997)
- [25] M.C. Kunde, R.S. Jangid, “Seismic Behavior of Isolated Bridges: A state of the art review”, Electronic Journal of Structural Engineering, (2003)